

Poster no	Presenter	Title	Topic
B16	Sümeyye Güney	MOLECULAR DOCKING AND SYNTHESIS OF NOVEL BIPHENYL-CHROMONE DERIVATIVES AS AMPK ACTIVATORS	Pharmaceutical Chemistry
B17	Diletta Liviabella	NEW INSIGHTS INTO COVALENT ENZYMATIC INHIBITION MEDIATED BY ELECTROPHILIC SELENIUM COMPOUNDS: THE CASE OF THE SARS-CoV-2 MAIN PROTEASE	Pharmaceutical Chemistry
B18	Ivayla Pantcheva	CRYSTAL STRUCTURE OF LITHIUM(I) COMPLEX OF THE ANTIBIOTIC LASALOCID	Pharmaceutical Chemistry
B19	Diana Cheshmedzhieva	AFFINITY OF THE POLYETHER IONOPHORE MONENSIN A TO BIND MONOVALENT METAL IONS: A DFT/PCM STUDY	Pharmaceutical Chemistry
B20	Radoslava Stamboliyska	MONONUCLEAR COPPER(II) COMPLEX OF MACROLIDE ANTIBIOTIC TILMICOSIN	Pharmaceutical Chemistry
B21	Radoslava Stamboliyska	DINUCLEAR COPPER(II) COMPLEXES OF MACROLIDE ANTIBIOTIC TILMICOSIN	Pharmaceutical Chemistry
B222	Erol Akgün	SYNTHESIS OF BENZIMIDAZOLE, BENZOTHAZOLE, BENZOFURANE AND NAPHTHOFURANE DERIVATIVES OF AMINOTHIAZOLES	Pharmaceutical Chemistry
B23	Nagihan Faydalı	STUDIES ON ANTIMICROBIAL PROPERTIES OF SOME BENZOXAZOLES	Pharmaceutical Chemistry
B24	Nagihan Faydalı	SYNTHESIS AND STRUCTURE ELUCIDATION OF SOME BENZOXAZOLE DERIVATIVES	Pharmaceutical Chemistry
B25	Selen Gurkan-Alp	SYNTHESIS OF SOME NOVEL SCHIFF BASES INCORPORATED WITH INDIAZOLE MOIETY	Pharmaceutical Chemistry
B26	Selen Gurkan-Alp	SYNTHESIS OF SOME NOVEL N'-((ARYL)METHYLENE)-1H-INDOLE-5-CARBOHYDRAZIDES	Pharmaceutical Chemistry
B27	Mehmet Alp	SYNTHESIS OF SOME NOVEL 4-(1H-BENZIMIDAZOL-1-YL)-N'-BENZYLIDENEBENZOHYDRAZIDE DERIVATIVES	Pharmaceutical Chemistry
B28	Ural Ufuk Demirel	DETERMINATION OF NOVEL UREA AND SULFONAMIDE DERIVATIVES OF ISATIN SCHIFF BASES AS POTENTIAL RECEPTOR TYROSINE KINASE INHIBITOR BY MOLECULAR DOCKING STUDIES.	Pharmaceutical Chemistry
B29	Dilay Kahvecioglu	THE EFFECT OF COX-2 INHIBITORS ON ACETYLCHOLINE ESTERASE IN TREATMENT OF ALZHEIMER'S DISEAS	Pharmaceutical Chemistry
B30	Ayça Dedeoğlu Erdoğan	SOME NEW 3,5 DISUBSTITUTED 1,3,4-OXADIAZOLE DERIVATIVES WITH IN VITRO ANTI-INFLAMMATORY ACTIVITY	Pharmaceutical Chemistry
B31	Sultan Butun Sengel	PREPARATION OF MICROPARTICLES FROM LAVENDER EXTRACT WITH HYDRO/SOLVOTHERMAL SYNTHESIS: CYTOTOXIC AND GENOTOXIC EFFECT ON CANCER CELL LINES	Pharmaceutical Chemistry
B32	Caner Arıkan	SYNTHESIS AND STANDARDIZATION OF AN IMPURITY OF ACETAMINOPHEN, DEVELOPMENT AND VALIDATION OF RELATED ULTRA-HIGH PERFORMANCE LIQUID CHROMATOGRAPHIC METHOD	Pharmaceutical Chemistry

MOLECULAR DOCKING AND SYNTHESIS OF NOVEL BIPHENYL-CHROMONE DERIVATIVES AS AMPK ACTIVATORS

²Güney S., ¹Ceylan-Ünlüsoy M.

¹Ankara University, Department of Pharmaceutical Chemistry, Ankara, Turkey, munlusoy@pharmacy.ankara.edu.tr,

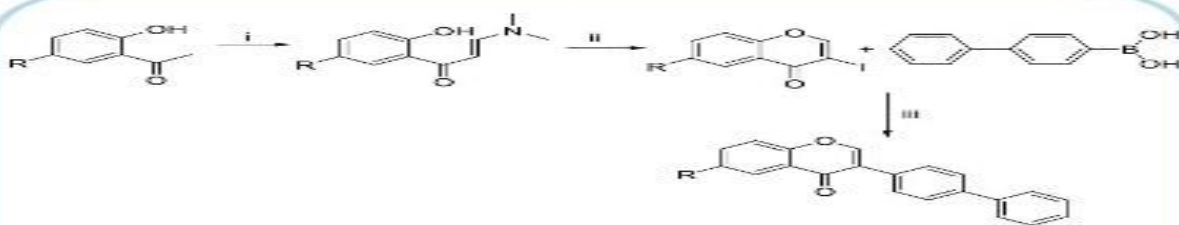
²Zonguldak Bülent Ecevit University, Department of Pharmaceutical Chemistry, Zonguldak, Turkey, sumeyye.guney@beun.edu.tr

Introduction

Adenosine monophosphate activated protein kinase (AMPK) works like an energy sensor and it is activated when the AMP/ATP or ADP/ATP ratio in the body increases in favor of AMP and ADP (1). It is involved in the regulation of carbohydrate, fat, protein metabolism, autophagy, and antioxidant defense during oxidative stress. AMPK has been a potential therapeutic target for many diseases from diabetes to cancer. Thus, various small molecules including flavonoids, which have chromone core, have been investigated and some of them have been found effective on AMPK (2). In addition, the biphenyl structure has been evaluated as an important pharmacophore in some AMPK activators (3). Inspired by these studies, we designed and synthesized some new biphenyl substituted chromone derivatives in order to test their AMPK activator and anticancer activities.

Materials and Methods

Molecular docking studies were carried out by using AutoDock Vina program. Substituted chromone ring is synthesized starting from various acetophenones. Then, Suzuki coupling reaction was carried out for the reaction of the chromone ring with the biphenyl structure as shown in the scheme below (4).



i: N, N-dimethylformamide dimethyl acetal, ii: CHCl_3 , I_2 , iii: $\text{Pd}(\text{PPh}_3)_4$, Na_2CO_3

Results

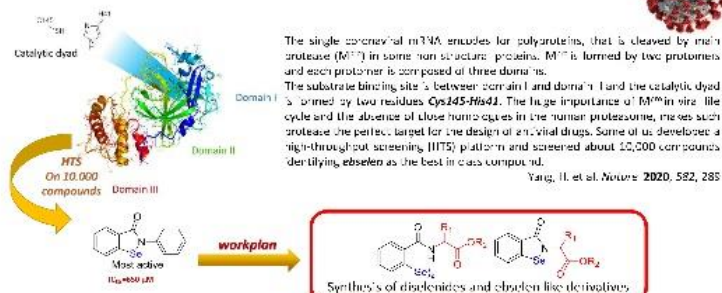
The structure of the synthesized compounds was elucidated by ¹H NMR, ¹³C NMR and mass spectral data. All spectral data were in accordance with assumed structures. The designed compounds have been shown to give similar docking poses to known AMPK activators.



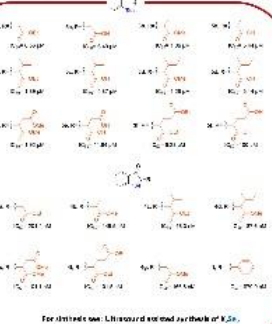


¹ Group of Catalysis Synthesis and Organic Green Chemistry, Department of Pharmaceutical Sciences, University of Perugia, Via del Liceo 1, 06100 Perugia Italy
PRESENTER: Diletta Liviabella ,diletta.liviabella@studenti.unipg.it

1

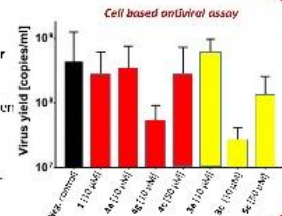


2



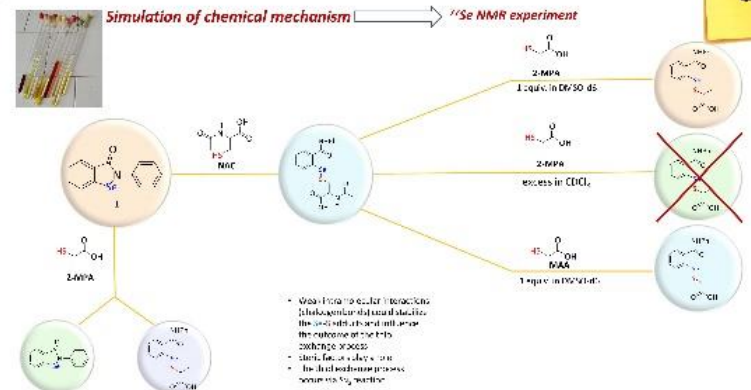
The best Mpro inhibitors were tested in a cellular model of viral replication:

- almost all observed like compounds showed some cytotoxicity
- **3c** is the best-in-class compound



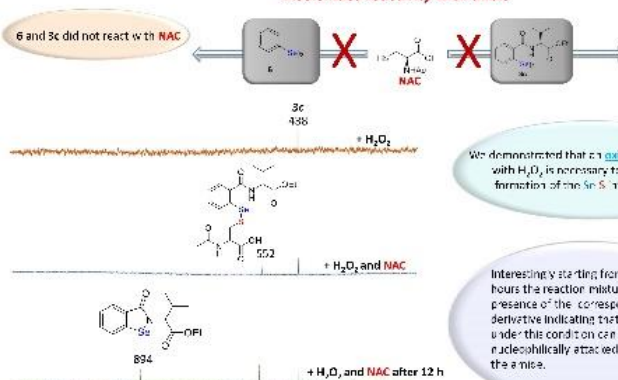
- 3c is the best-in-

3



4

□



We demonstrated that an [oxidative activation](#) with H_2O_2 is necessary to observe the formation of the Sn-S⁺ isomers *intra*.

Interestingly starting from **3c**, after 12 hours the reaction mixture evidenced the presence of the corresponding ebselen derivative indicating that the Se-S bond under this condition can be nucleophilically attacked by the nitrogen of the amine.

6

- Probably the reaction between ebselen like compound and Cys145 was a 5x, reaction
- When FBS and its derivatives enter in the cell they most probably interact immediately with GST and then the corresponding **Se 5 adduct** could interact with Mpro
- Diselenides are good antiviral compounds in the inhibition of SARS-CoV-2 in cellular test. Probably the stable **Se-Se** bond could be activated by a high concentration of ROS present in infected cells. There the formation of an electrophile **Se** could explained the reactivity between diselenides and Cys145.

More details can be found in: I. Sanchez, F. Mangano, A. I. Lopez, A. P. de, M. Gonzalez-Fabris, C. Simion, Y. Li, J. Kong, Y. Zhao, K. dos Santos Machado, A. Velasco Weill, G. Ciancio, V. Nascimento, A. Kula-Pocur, E. J. Leonidis, A. Yang, J. Sciannowski, K. Pyrr, C. Santi. 2020, DOI: 10.26434/chemrxiv-2020-250-x1





Crystal structure of lithium(I) complex of the antibiotic Lasalocid

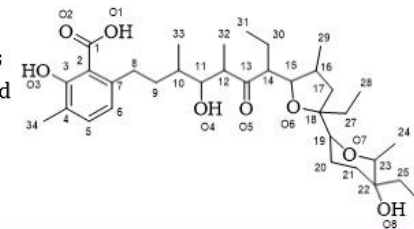
Pantcheva, I., Stamboliyska, R., Ugrinov, A.

Sofia University "St. Kl. Ohridski", Faculty of Chemistry and Pharmacy, Sofia, Bulgaria, ahip@chem.uni-sofia.bg

I. INTRODUCTION

Lasalocid acid (LasH) is a polyether ionophorous antibiotic and is applied as coccidostatic and food supplement. In addition, LasH and its derivatives are active against some bacterial strains and tumour cells. The known structures of Lasalocid with monovalent metal ions revealed that the antibiotic forms complex species of various composition, serving mainly as a polydentate ligand. Crystallographic studies demonstrated that Lasalocid does not possess a uniform coordination mode towards monovalent metal cations.

In the present study we report the crystal structure and spectral properties of a new lithium(I) complex of Lasalocid.



II. METHODOLOGY:

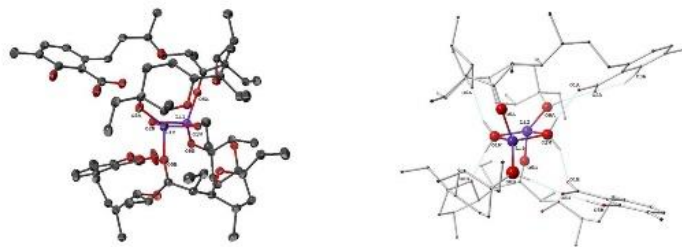
Synthetic conditions:

molar LiOH:LasH ratio 5:1 in aqueous/Et₂O solution

X-ray diffraction on single crystals isolated from organic phase
IR, ESI-MS spectrometry

III.1. RESULTS & DISCUSSION – X-ray crystallography

- ✓ **Composition** - [Li₂(μ₂-Las₂)(μ₂-H₂O)₂]
- ✓ **Cell** - four dinuclear lithium(I) complexes of Lasalocid - one of them is the asymmetric unit of the structure and the other 3 are symmetry related images
- ✓ **Dinuclear structure** - core unit of Li₂O₄
- ✓ **Both metal centres** - bridged by **two water molecules** (O1W, O2W) - bidentate ligands
- ✓ **Two Lasalocidate ligands** complete the coordination sites of the metal centers
- ✓ **Geometry of the Li₂O₂ chromophore** - a planar slightly distorted square



Selected Bond Lengths (Å)

Li1-O1W	1.964(8)	Li2-O1W	1.965(9)
Li1-O2W	2.033(8)	Li2-O2W	2.034(9)
Li1-O5A	1.912(9)	Li2-O5B	1.934(9)
Li2-O8A	1.903(10)	Li1-O8B	1.907(9)

Selected Bond Angles (°)

Li1-O1W-Li2	94.1(4)	O1W-Li1-O2W	88.0(3)
Li1-O2W-Li2	90.0(3)	O1W-Li2-O2W	87.9(4)

III.2. RESULTS & DISCUSSION – Spectral properties of Li(I) complex of Lasalocid

IR spectroscopy – Functional groups:

Lasalocid acid – hydroxyl (ν_{OH}, 3440 cm⁻¹), carbonyl (ν_{C=O}, 1714 cm⁻¹), carboxyl (ν_{C=O}, 1654 cm⁻¹), benzene (ν_{C=C}, 1615 cm⁻¹), carboxyl (δ_{OH}, 1417 cm⁻¹), hydroxyl (ν_{C-O}, 1245 cm⁻¹)

Li(I) complex – hydroxyl (ν_{OH}, 3370 cm⁻¹), carboxylate anion (ν_{COO}^{as}, 1574 cm⁻¹; ν_{COO}^s, 1428 cm⁻¹)

ESI-MS spectroscopy – Molecular ions:

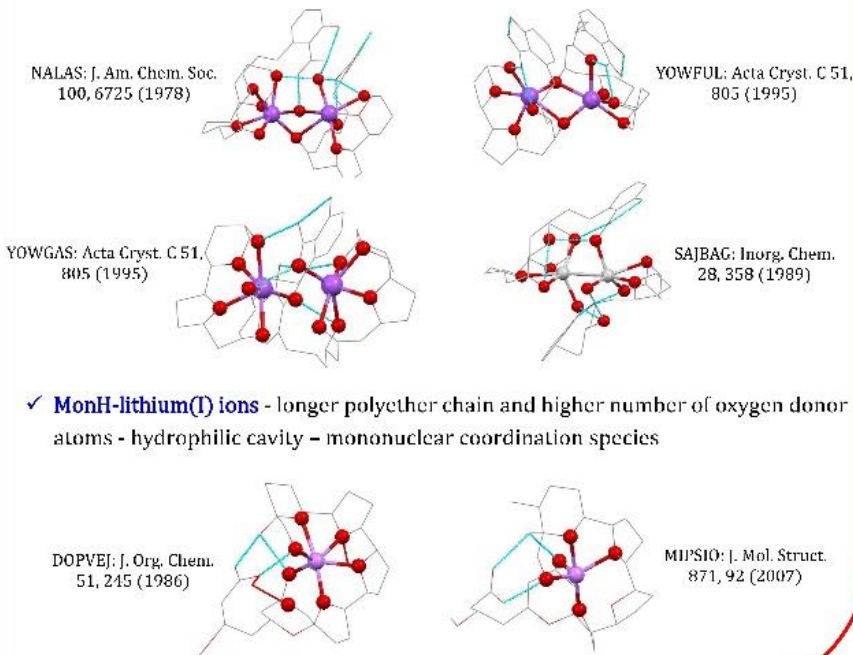
[Li₂Las₂Li]⁺ and [Li₂Las₂Na]⁺

IV. CONSLUCIONS

- ✓ A novel neutral dinuclear lithium(I) complex of Lasalocid acid
 - ✓ Fundamental knowledge in coordination chemistry of the smallest polyether ionophore and its binding ability towards alkali metal ions.
 - ✓ High flexibility of Lasalocid acid enables the smallest alkali metal cation to be successfully captured.
 - ✓ In order a lithium(II) bis-Lasalocidate complex to be formed, a dinuclear Li-containing core is a necessity.
- Our findings may lay ground for future studies evaluating the coordination behavior of lithium(I) ions and their potential impact on structural diversity.

III.3. RESULTS & DISCUSSION – Novel coordination mode of Lasalocid

- ✓ **Li(I) complex** – the first example of a clear formation of dinuclear complex of LasH
- ✓ **Structure** – “sandwich” type
- ✓ **LasH-alkali metal ions (Na, Ag, Tl)** – LasH is a polydentate ligand – monomer, dimer or polymer species without well defined hydrophilic cavity



Affinity of the polyether ionophore Monensin A to bind monovalent metal ions: A DFT/PCM study

Diana Cheshmedzhieva^a, Todor Dudev^a, Radoslava Dimitrova^b, Peter Dorkov^c, Ivayla Pantcheva^b

^aLaboratory of Computational Chemistry and Spectroscopy, Faculty of Chemistry and Pharmacy, "St. Kl. Ohridski" University of Sofia, Bulgaria

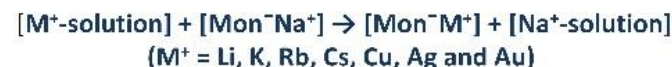
^bLaboratory of Biocoordination and Bioanalytical Chemistry, Faculty of Chemistry and Pharmacy, "St. Kl. Ohridski" University of Sofia, Bulgaria

^cBiomet Ltd., Research & Development Department, Peshtera, Bulgaria

*Corresponding author: valentinova@chem.uni-sofia.bg

Abstract

The affinity of monensin A to bind monovalent metal cations was evaluated by means of density functional theory (DFT) combined with polarizable continuum model (PCM) computations. The effect of various factors which may render on complex formation between monensinate A anion and Group IA and IB metal ions was accessed. Competition between Na⁺ taken as a reference and monovalent metal cations was estimated using the free Gibbs energy for substituting the ligand-bound Na⁺ with its rival ions in the process



The calculations revealed that the decrease in size of cations accompanied by an increase of their accepting ability enhances the metal selectivity towards ligand donor atoms. In the gas-phase the affinity of monensinate A decreases in the order Cu⁺ > Li⁺ > Na⁺ > Au⁺ > Ag⁺ > K⁺ > Rb⁺ > Cs⁺. The complex formation can be manipulated by changing the solvent used. The polyether ionophore selectively binds Na⁺ ions in polar solvents but could become Li⁺ or Cu⁺-selective in low-polarity solvents.

DFT/PCM calculations

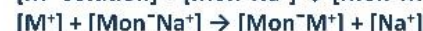
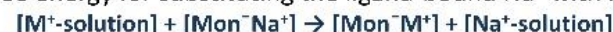
All calculations were performed using Gaussian 09 package of programs.

All the structures were fully optimized in the gas phase at B3LYP/6-31+G(d,p) level of theory yielding the respective electronic energies, E_{elect} of the studied species.

SDD basis set and effective core potential were used for heavier metal ions in the series such as Rb⁺, Cs⁺, Ag⁺ and Au⁺.

Reaction modeled

The competition between the group IA and IB cations and Na⁺ (taken as a reference) in monensinate A can be expressed in terms of the Gibbs free energy for substituting the ligand-bound Na⁺ with its rival cations:



$$\Delta G^1 = \Delta E_{\text{elect}} + \Delta E_T - T\Delta S$$

$$\Delta G^E = \Delta G^1 + \Delta G^E_{\text{sol}} ([\text{Mon}^-\text{M}^+]) + \Delta G^E_{\text{sol}} ([\text{Na}^+-\text{solution}]) - \Delta G^E_{\text{sol}} ([\text{Mon}^-\text{Na}^+]) - \Delta G^E_{\text{sol}} ([M^+-\text{solution}])$$



Figure 1. Optimized geometry of [Mon⁻Na⁺] complex at the B3LYP/6-31+G(d,p) level of theory. Color scheme: C – green, O – red, H – light grey, Na – purple.

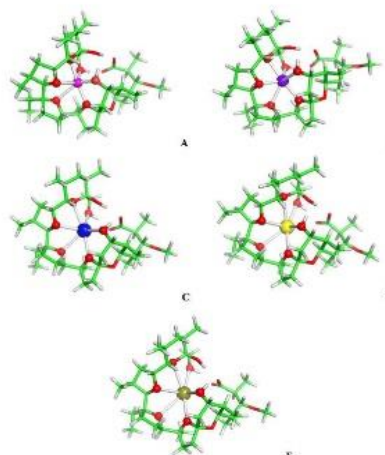


Figure 2. B3LYP/6-31+G(d,p) fully optimized structures of monensinate A anion bound to (A) Li⁺, (B) Na⁺, (C) K⁺, (D) Rb⁺ and (E) Cs⁺. Color scheme: C – green, O – red, H – light grey, Li – magenta, Na – purple, K – blue, Rb – yellow, Cs – deep olive.

Table 1. Competition between sodium compound and monovalent metal cations (Å) and ions radii^a (Å) (R_{ion} 20^b Crystallog).

Monovalent cations	[MonNa ⁺]	
	Na ⁺	Li ⁺
Na-O ₁	2.11	2.11
Na-O ₂	2.11	2.11
Na-O ₃	2.00	2.00
Na-O ₄	2.11	2.11
Na-O ₅	2.11	2.11
Na-O ₆	2.11	2.11
Na-O ₇	2.11	2.11
Na-O ₈	2.11	2.11
Na-O ₉	2.11	2.11
Na-O ₁₀	2.11	2.11
Na-O ₁₁	2.11	2.11
Na-O ₁₂	2.11	2.11
Na-O ₁₃	2.11	2.11
Na-O ₁₄	2.11	2.11
Na-O ₁₅	2.11	2.11
Na-O ₁₆	2.11	2.11
Na-O ₁₇	2.11	2.11
Na-O ₁₈	2.11	2.11
Na-O ₁₉	2.11	2.11
Na-O ₂₀	2.11	2.11
Na-O ₂₁	2.11	2.11
Na-O ₂₂	2.11	2.11
Na-O ₂₃	2.11	2.11
Na-O ₂₄	2.11	2.11
Na-O ₂₅	2.11	2.11
Na-O ₂₆	2.11	2.11
Na-O ₂₇	2.11	2.11
Na-O ₂₈	2.11	2.11
Na-O ₂₉	2.11	2.11
Na-O ₃₀	2.11	2.11
Na-O ₃₁	2.11	2.11
Na-O ₃₂	2.11	2.11
Na-O ₃₃	2.11	2.11
Na-O ₃₄	2.11	2.11
Na-O ₃₅	2.11	2.11
Na-O ₃₆	2.11	2.11
Na-O ₃₇	2.11	2.11
Na-O ₃₈	2.11	2.11
Na-O ₃₉	2.11	2.11
Na-O ₄₀	2.11	2.11
Na-O ₄₁	2.11	2.11
Na-O ₄₂	2.11	2.11
Na-O ₄₃	2.11	2.11
Na-O ₄₄	2.11	2.11
Na-O ₄₅	2.11	2.11
Na-O ₄₆	2.11	2.11
Na-O ₄₇	2.11	2.11
Na-O ₄₈	2.11	2.11
Na-O ₄₉	2.11	2.11
Na-O ₅₀	2.11	2.11
Na-O ₅₁	2.11	2.11
Na-O ₅₂	2.11	2.11
Na-O ₅₃	2.11	2.11
Na-O ₅₄	2.11	2.11
Na-O ₅₅	2.11	2.11
Na-O ₅₆	2.11	2.11
Na-O ₅₇	2.11	2.11
Na-O ₅₈	2.11	2.11
Na-O ₅₉	2.11	2.11
Na-O ₆₀	2.11	2.11
Na-O ₆₁	2.11	2.11
Na-O ₆₂	2.11	2.11
Na-O ₆₃	2.11	2.11
Na-O ₆₄	2.11	2.11
Na-O ₆₅	2.11	2.11
Na-O ₆₆	2.11	2.11
Na-O ₆₇	2.11	2.11
Na-O ₆₈	2.11	2.11
Na-O ₆₉	2.11	2.11
Na-O ₇₀	2.11	2.11
Na-O ₇₁	2.11	2.11
Na-O ₇₂	2.11	2.11
Na-O ₇₃	2.11	2.11
Na-O ₇₄	2.11	2.11
Na-O ₇₅	2.11	2.11
Na-O ₇₆	2.11	2.11
Na-O ₇₇	2.11	2.11
Na-O ₇₈	2.11	2.11
Na-O ₇₉	2.11	2.11
Na-O ₈₀	2.11	2.11
Na-O ₈₁	2.11	2.11
Na-O ₈₂	2.11	2.11
Na-O ₈₃	2.11	2.11
Na-O ₈₄	2.11	2.11
Na-O ₈₅	2.11	2.11
Na-O ₈₆	2.11	2.11
Na-O ₈₇	2.11	2.11
Na-O ₈₈	2.11	2.11
Na-O ₈₉	2.11	2.11
Na-O ₉₀	2.11	2.11
Na-O ₉₁	2.11	2.11
Na-O ₉₂	2.11	2.11
Na-O ₉₃	2.11	2.11
Na-O ₉₄	2.11	2.11
Na-O ₉₅	2.11	2.11
Na-O ₉₆	2.11	2.11
Na-O ₉₇	2.11	2.11
Na-O ₉₈	2.11	2.11
Na-O ₉₉	2.11	2.11
Na-O ₁₀₀	2.11	2.11

^a Data extracted from the Cambridge Structural Database (CSD) for the Na⁺ ion. ^b Data extracted from the Cambridge Structural Database (CSD) for the Li⁺ ion.

Table 2. Structural and electronic characteristics of Group IA and IB metal cations with the ligand monensinate A.

Metal ion	Coordination number	Average M-O distance (Å)	Charge transfer to the metal (e ⁻)	Charge transfer from the metal (e ⁻)
Li ⁺	6	2.05	0.00	0.00
Na ⁺	6	2.05	0.00	0.00
K ⁺	6	2.05	0.00	0.00
Rb ⁺	6	2.05	0.00	0.00
Cs ⁺	6	2.05	0.00	0.00
Cu ⁺	6	2.05	0.00	0.00
Ag ⁺	6	2.05	0.00	0.00
Au ⁺	6	2.05	0.00	0.00

^a Data extracted from the Cambridge Structural Database (CSD) for the Na⁺ ion. ^b Data extracted from the Cambridge Structural Database (CSD) for the Li⁺ ion.

Concluding remarks

The calculations performed reveal the following key determinants of the monovalent metal selectivity in monensinate A anion:

- The metal ion radius: smaller size cations, with higher positive charge density, are more competitive than their bulkier counterparts;
- The metal cation charge accepting ability: increasing the metal charge accepting ability, especially for *d*-elements, which translates into increased affinity toward the surrounding ligands (donor atoms), enhances the metal ion selectivity;
- The dielectric properties of the medium: low-polarity solvents favor the smaller ions possessing high ligand affinity (Li⁺ and Cu⁺); in polar solvents, characterized with high dielectric constants, the competitiveness of the medium-size cations, particularly Na⁺, increases.

The size of the internal cavity appears to be a secondary factor of the metal selectivity as the pore is relatively flexible and adaptable to certain extent to the spatial requirements of the incoming metal cations.

Note that the role of the solvent in governing the metal affinity of monensinate A anion is evaluated for the first time here (to the best of our knowledge). Our results imply that the metal selectivity of monensin A can be manipulated by changing the solvent used: the polyether host selectively binds Na⁺ in polar solvents (methanol and water) but could become Li⁺ or Cu⁺-selective in low-polarity solvents such as alkyl ethers, hydrocarbons and their halogenated derivatives.

Acknowledgements

The authors are thankful for the support by National Science Fund, Bulgarian Ministry of Education and Science (contract № KP-06-H29/3).



MONONUCLEAR COPPER(II) COMPLEX OF MACROLIDE ANTIBIOTIC TILMICOSIN

Stamboliyska, R., Petkov, N., Pantcheva, I., Stoykova, S., Stoyanova, R., Kukeva, R., Simova, S.
Sofia University "St. Kl. Ohridski", Faculty of Chemistry and Pharmacy, Sofia, Bulgaria, radoslava.dimitrova@abv.bg

I. INTRODUCTION

The semi-synthetic 16-membered macrolide antibiotic Tilmicosin is an effective drug in veterinary medicine treating pulmonary infections caused by bacterial strains. On the other hand, it is well known that the modification of biologically active compounds by complexation processes may enhance the activity of the parent molecules. In the present study we discuss the ability of Tilmicosin to bind Cu(II) ions in aqueous solutions and the properties of the complex species formed.

II. METHODOLOGY:

Synthetic conditions:

molar metal-to-ligand ratio 1:2 in aqueous solution at pH 11

UV-VIS spectroscopy in solution

IR spectroscopy in solid state

EPR in solution and in solid state

NMR in solution and in solid state

Quantum chemical calculations – absorption energies and EPR parameters

Antibacterial activity of compounds of interest:

double layer agar hole diffusion method

Gram-positive bacteria: *B. subtilis*, *B. cereus*, *K. rhizophila*

III.1. RESULTS & DISCUSSION - SYNTHESIS

Mixing aqueous solutions of Tilmicosin (0, 1 mmol) and CuCl₂·2H₂O (0,05 mmol), followed by increasing of pH by KOH undergoes the formation of violet precipitates, which were filtered off and dried (yield: 59%).

III.2. RESULTS & DISCUSSION – UV-VIS & IR DATA

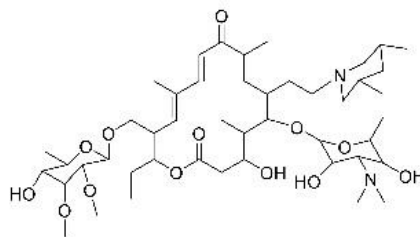
The absorbance of isolated Cu(II)-containing Tilmicosinate species was characterized in EtOH (UV-VIS) and acetone (VIS) solutions.

compound	solvent	λ [nm]	ϵ [M ⁻¹ cm ⁻¹]	λ [nm]	ϵ [M ⁻¹ cm ⁻¹]
Tilmicosin	EtOH	285	18215	-	-
Violet complex	EtOH	285	37380	520	108
	acetone	-	-	510	94

No significant changes in the IR spectrum of Violet complex as compared to the IR data of Tilmicosin.

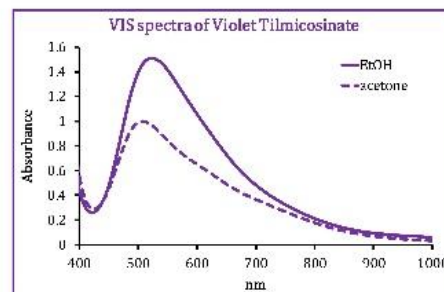
IV. CONSLUCIONS

The macrolide antibiotic Tilmicosin forms a mononuclear Violet complex with Cu(II) ions, where two deprotonated ligand anions are bound in trans-position to the metal(II) center. The structure of novel species was elucidated using a set of spectroscopic studies and quantum chemical calculations. The antimicrobial assays revealed that copper(II) species are better agents against Gram-positive microorganisms as compared to the non-coordinated parent compound.



III.4. RESULTS & DISCUSSION – NMR DATA

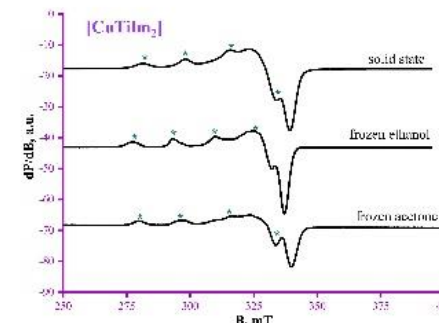
To distinguish between the N-donor atoms, coordinated to copper(II) centers, we performed a NMR titration in acetone-d₆. Data revealed that the chemical shift belonging to the N,N-dimethylamine groups in the mycaminoose fragment is mainly affected due to the coordination of Cu(II) cations. Thus it was proved that the mycaminoose is the solely substituent binding transition metal(II) ions.



III.3. RESULTS & DISCUSSION – EPR DATA

The EPR parameters of Cu(II)-Tilmicosinate complex were determined in solid state and EtOH / acetone solutions at 100 K. The parameters α^2 and G account for ionic bond character ($\alpha^2 > 0.5$) and absence of exchange interaction between metal(II) centers ($G > 4$).

state	$g_{ }$	$A_{ }$ [G]	g_{\perp}	α^2	G
Solid	2.202	171	2.036	0.70	5.61
EtOH solution	2.236	158	2.037	0.70	6.38
Acetone solution	2.214	170	2.038	0.71	5.63



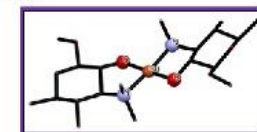
III.5. RESULTS & DISCUSSION – DFT study

Geometry optimization of the complex in the ground state was performed with B3LYP/6-31G* in vacuo and in implicit solvent acetone using the polarizable continuum model with Gaussian 16 software. The bond distances and bond angles for the optimized structure, as well as the d-d* transitions (calculated with TD-B3LYP/6-31G*/PCM(acetone)) and EPR parameters (calculated with the ORCA software package B3LYP/6-31G*/Wachters+*f* in vacuo) corroborate very well with the experimental data observed.

calculated	λ [nm]	Cu-N [Å]	Cu-O [Å]	$g_{ }$	$A_{ }$ [G]	g_{\perp}
Violet complex	530	2.08	1.86	2.22	188	2.06

III.6. RESULTS & DISCUSSION – STRUCTURE OF THE VIOLET COMPLEX OF TILMICOSIN

The Violet complex of Tilmicosin does not easily crystallize. Based on experimental and theoretical studies performed, we assume that the complex formed is of composition [CuTilm₂]. The Tilmicosinate ligands act in a bidentate coordination manner, forming a [CuN₂O₂] chromophore. The species formed represent a mononuclear copper(II) complex coordinated to two deprotonated ligand anions.



III.7. RESULTS & DISCUSSION – BIOLOGICAL ACTIVITY

The ability of Tilmicosin and its mononuclear complex to inhibit the visible growths of Gram-positive microorganisms was studied against the panel of three bacterial strains.

Bacteria	<i>K. rhizophila</i> , MIC		<i>B. Subtilis</i> , MIC		<i>B. cereus</i> , MIC	
Compound	μg/mL	μM	μg/mL	μM	μg/mL	μM
Tilmicosin	0.25	0.28	2	2.3	1	1.1
Violet complex	0.25	0.14	2	1.1	1	0.5

V. ACKNOWLEDGEMENTS

The present research was supported by a grant of Sofia University (Contract 80-10-143/2021).



DINUCLEAR COPPER(II) COMPLEXES OF MACROLIDE ANTIBIOTIC TILMICOSIN

Stamboliyska, R., Petkov, N., Pantcheva, I., Stoykova, S., Stoyanova, R., Kukeva, R., Simova, S.

Sofia University "St. Kl. Ohridski", Faculty of Chemistry and Pharmacy, Sofia, Bulgaria, radoslava.d.dimitrova@abv.bg

I. INTRODUCTION

The macrolide antibiotic Tilmicosin is a semi-synthetic drug applied in veterinary medicine in case of bacterial infections of various origin. Here we present data on its ability to bind Cu(II) ions in non-aqueous solutions and on the properties of complex species formed.

II. METHODOLOGY:

Synthetic conditions:

molar metal-to-ligand ratio 1:1 in acetone solution

$\text{CuCl}_2 \cdot 2\text{H}_2\text{O} / \text{Cu}(\text{NO}_3)_2 \cdot 3\text{H}_2\text{O}$

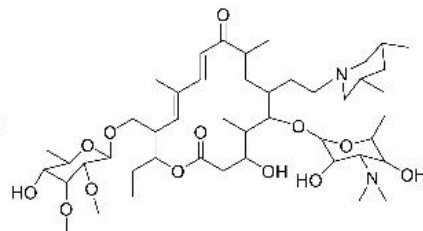
UV-VIS, EPR, NMR spectroscopy

Quantum chemical calculations - DFT

Antibacterial activity of compounds tested:

double layer agar hole diffusion method

Gram-positive bacteria: *B. subtilis*, *B. cereus*, *K. rhizophila*

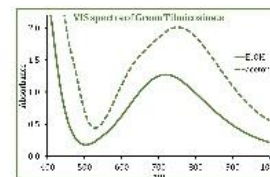
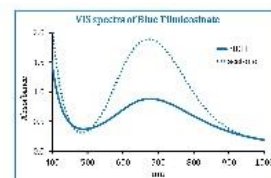


III.1. RESULTS & DISCUSSION - SYNTHESIS

Mixing acetone solutions of Tilmicosin (0,1 mmol) and copper(II) salt (0,1 mmol) leads to the formation of blue $(\text{Cu}(\text{NO}_3)_2 \cdot 3\text{H}_2\text{O})$ or green $(\text{CuCl}_2 \cdot 2\text{H}_2\text{O})$ transparent solutions. The slow addition of reaction mixtures to ether affords the precipitation of corresponding solid phases, which were filtered off and dried (yield: blue – 75%; green - 90%).

III.2. RESULTS & DISCUSSION – UV-VIS DATA

The UV-VIS behaviour of isolated Cu(II)-containing Tylosinate species was characterized in EtOH (UV-VIS) and acetone (VIS) solutions.

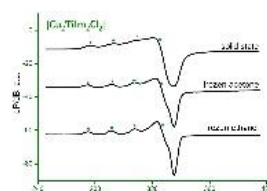
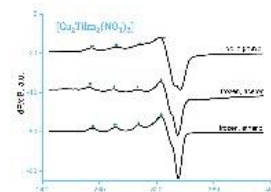


compound	solvent	λ [nm]	ϵ [$\text{M}^{-1}\text{cm}^{-1}$]	λ [nm]	ϵ [$\text{M}^{-1}\text{cm}^{-1}$]
Tilmicosin	EtOH	285	18215	-	-
Blue complex	EtOH	285	33251	676	97
	acetone	-	-	670	150
Green complex	EtOH	285	38421	716	125
	acetone	-	-	755	170

III.3. RESULTS & DISCUSSION – EPR DATA

The EPR parameters of Cu(II)-Tilmicosinate complexes were evaluated in solid state and EtOH / acetone solutions at 100 K. The parameters α^2 and G account for ionic bond character ($\alpha^2 > 0.5$) and absence of exchange interaction between metal(II) centers ($G > 4$).

complex	state	$g_{ }$	$A_{ }$ [G]	g_{\perp}	α^2	G
Blue complex	Solid	2.249	175	2.059	0.76	4.35
	EtOH solution	2.235	155	2.047	0.69	5.20
	Acetone solution	2.262	170	2.054	0.76	5.02
Green complex	Solid	2.251	164	2.045	0.73	5.82
	EtOH solution	2.252	164	2.045	0.73	5.85
	Acetone solution	2.252	164	2.045	0.73	5.85

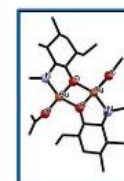
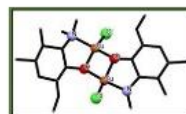


III.4. RESULTS & DISCUSSION – NMR DATA

The NMR titration in acetone- d_6 confirmed that the chemical shift belonging to the methyl groups bound to N-atom from mycaminoso fragment is mainly affected due to the coordination of Cu(II) cations.

III.5. RESULTS & DISCUSSION – DFT STUDY

Geometry optimization of the complex in the ground state was performed with Gaussian 16 software (B3LYP/6-31G* in vacuo and in implicit solvent acetone using the polarizable continuum model). The bond distances and bond angles for the optimized structure, as well as the d-d* transitions (TD-B3LYP/6-31G*/PCM(acetone)) and EPR parameters (ORCA software package B3LYP/6-31G*/Wachters+f in vacuo) are in a good agreement with the experimental data observed.



	calculated	λ [nm]	Cu-N [Å]	Cu-O [Å]	Cu-O-Cu [°]	Cu-Cl [Å]	$g_{ }$	g_{\perp}
Blue complex		684	2.0382	1.9031 / 1.9164	99.40	-	2.20	2.12
			2.0473	1.9075 / 1.9556	98.95			
				1.9555 / 1.9555				
Green complex		735	2.0378	1.9083 / 1.9170	99.19	2.2232	2.19	2.11
			2.0492	1.9459 / 1.9476	98.83	2.2232		

III.6. RESULTS & DISCUSSION – BIOLOGICAL ACTIVITY

Bacteria	<i>K. rhizophila</i> , MIC		<i>B. Subtilis</i> , MIC		<i>B. cereus</i> , MIC	
Compound	$\mu\text{g/mL}$	μM	$\mu\text{g/mL}$	μM	$\mu\text{g/mL}$	μM
Tilmicosin	0.25	0.28	2	2.3	1	1.1
Blue complex	1	0.50	1	0.50	1	0.50
Green complex	0.5	0.26	< 2	< 1	1	0.50

V. ACKNOWLEDGEMENTS: The present research was supported by a grant of Sofia University (Contract 80-10-143/2021).

IV. CONSLUCIONS

Macrolide antibiotic Tilmicosin complexes with Cu(II) nitrate or chloride in non-aqueous solutions. Two bidentate Tilmicosinate anions serves as a bridge binding two metal centers via the oxygen atom. The fourth place in the inner coordination sphere of the metal(II) cations is occupied by nitrate (blue complex) or chloride (green complex) ions. The ligand plays a dual function, forming the main chromophore unit of $[\text{Cu}_2\text{N}_2\text{O}_2]$ or $[\text{Cu}_2\text{N}_2\text{O}_2\text{Cl}_2]$, respectively.

STUDIES ON ANTIMICROBIAL PROPERTIES OF SOME BENZOXAZOLES

Faydalı, N., ¹Temiz Arpacı, O., ²Kaymaklı, G., ³Sakat, A. S.
¹Selek University, Department of Pharmaceutical Chemistry, Konya, Turkey, naghlan.faydali@selek.edu.tr
²Ankara University, Department of Pharmaceutical Chemistry, Ankara, Turkey,
³Trakya University, Department of Medical Microbiology, Edirne, Turkey,
⁴Trakya University, Department of Pharmaceutical Microbiology, Edirne, Turkey.

INTRODUCTION

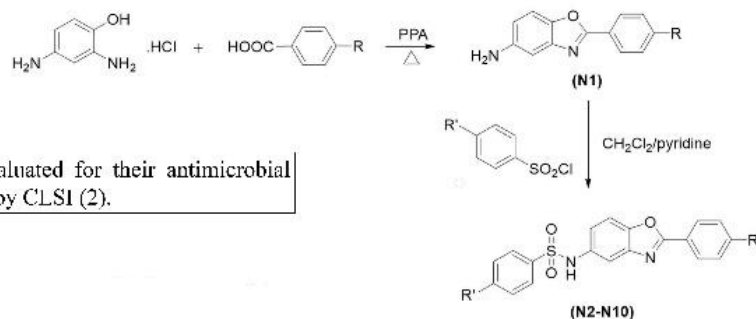
Infectious diseases caused by bacteria and fungi are still one of the most important threats to public health despite great advances in pharmaceutical and medicinal chemistry. Benzoxazole compounds are important medicinal chemistry because of their wide range of biological activities including antimicrobial activity (1).

In this study, in comparison with several control drugs the newly synthesized compounds were evaluated for their antibacterial and antifungal activity against standard strains and drug-resistant isolates.

MATERIALS AND METHODS

General procedure for obtaining 5-Amino-2-(p-substituted phenyl)benzoxazole (N1): 1 mmol 2,4-diaminophenol dihydrochloride and 1 mmol p-substituted benzoic acid were reacted in the presence of PPA (polyphosphoric acid) at 160-190 °C for about 3 h. The intermediate product obtained as a result of the reaction was taken to ice and mixed. After mixing well, it was neutralized with 10% NaOH and filtered. Finally, after the product was cleaned with activated charcoal, it was dissolved with ethanol and recrystallized.

General procedure for obtaining 2-(p-substitutedphenyl)-5-[(4-substitutedphenyl)sulfonylamido] benzoxazoles (N2-N10): Target compounds was obtained by reaction of 5-amino-2-(p-substitutedphenyl)benzoxazoles with p-substituted-benzenesulfonyl chloride in the presence of dichloromethane and pyridine. Target products were crystallized from ethanol.



The benzoxazoles (compounds 2-10) were evaluated for their antimicrobial activity with microdilution technique described by CLSI (2).

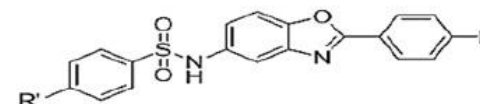
REFERENCES

1. Erol M, Celik I, Temiz Arpacı O, Kaymaklı O, Oktan S (2020). J Biomol Struct Dyn, 1-12.
2. Clinical and Laboratory Standards Institute (CLSI) (formerly NCCLS): Reference method for broth dilution antifungal susceptibility testing yeast: approved standard, M27-A3. Clinical and Laboratory Standards Institute, 940 West Valley Road, Wayne, Pennsylvania, USA, 2006.

RESULTS & DISCUSSION

Microbiological results showed that some benzoxazoles derivatives compounds possess an antimicrobial activity having MIC values of 32-512 µg/ml against the tested microorganisms.

Table 1. Antimicrobial activity results (MIC µg/ml) of the compounds with the standart drugs



Compound	R'	R	Gram positive bacteria				Gram negative bacteria				Fungus	
			S. a.	S. a.*	E. f.	E. f.*	E. c.	E. c.*	P. a.	P. a.*	C. a.	C. a.*
N2	-F	-C ₂ H ₅	32	256	256	128	128	256	128	256	128	256
N3	-NO ₂	-C ₂ H ₅	256	256	256	128	256	256	128	256	256	256
N4	-CH ₃	-C ₂ H ₅	256	256	256	128	128	256	128	256	256	128
N5	-Cl	-C ₂ H ₅	128	256	256	128	256	256	128	256	256	256
N6	-H	-F	256	256	256	128	256	256	128	256	128	128
N7	-F	-F	256	256	256	128	256	256	128	256	256	128
N8	-Br	-F	256	256	256	128	256	256	128	128	128	128
N9	-CH ₃	-F	256	256	256	128	128	128	128	256	256	256
N10	OCH ₃	-F	32	256	256	128	256	128	128	256	256	128
Ampicillin			0,5	>16	2	>16	8	>16	-	-	-	-
Vancomycin			0,5	2	1	>8	-	-	-	-	-	-
Gentamycin			0,25	>16	4	>8	0,5	>8	0,5	>8	-	-
Ciprofloxacin			0,5	>16	2	>4	0,0156	>2	0,125	>2	-	-
Cefotaxime			1	>16	-	-	0,125	>8	8	-	-	-
Fluconazole			-	-	-	-	-	-	-	-	0,125	>4
Amphotericin B			-	-	-	-	-	-	-	-	0,5	0,5

S. a.: Staphylococcus aureus ATCC 29213; S. a.*: Methicillin resistant S. aureus; E. f: Enterococcus faecalis ATCC 29212; E. f.*: Vancomycin resistant E. faecalis; E. c.: Escherichia coli, ATCC 25922; E. c.*: E. coli isolate P. a.: Pseudomonas aeruginosa ATCC 27853; P. a.*: P. aeruginosa isolate (gentamicin resistant); C. a: Candida albicans ATCC 10231; C. a.*: C. albicans isolate.

SYNTHESIS AND STRUCTURE ELUCIDATION OF SOME BENZOXAZOLE DERIVATIVES

Faydalı, N., Temiz Arpaçlı, O.,
Silecik University, Department of Pharmaceutical Chemistry, Konya, Turkey,
nagihan.faydali@silecik.edu.tr
Ankara University, Department of Pharmaceutical Chemistry, Ankara, Turkey.

INTRODUCTION

The number of life-threatening infections caused by the multi-drug resistant microorganisms has reached an alarming level in hospitals and the community [1-2]. Because of misuse of antibiotics bacteria have become antibiotic-resistant that may result in a potential global health crisis in the near future.

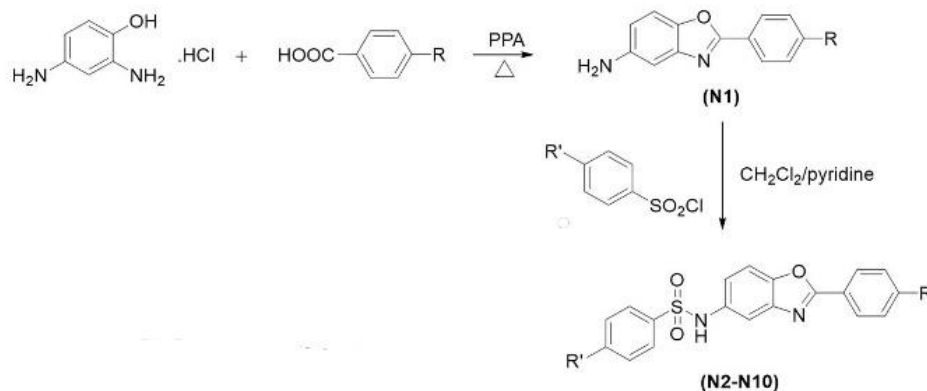
Benzoxazoles is an important ring system as it can easily interact with biopolymers in the organism as ring equivalents of purine bases of adenine and guanine, which are in the structure of nucleic acids [3]. So that benzoxazoles showed several activities including antibiotic, antimicrobial, antiviral, topoisomerase I and II inhibitors and antitumor activities.

In this study, novel 2-(p-substitutedphenyl)-5-[(4-substitutedphenyl)sulfonylamido] benzoxazoles were synthesized (Scheme) and structures of all compounds were elucidated by $^1\text{H-NMR}$, $^{13}\text{C-NMR}$ and MASS dates by this study (Table).

MATERIALS AND METHODS

General procedure for obtaining 5-Amino-2-(p-substituted phenyl)benzoxazole (N1): 1 mmol 2,4-diaminophenol dihydrochloride and 1 mmol p-substituted benzoic acid were reacted in the presence of PPA (polyphosphoric acid) at 160-190 °C for about 3 h. The intermediate product obtained as a result of the reaction was taken to ice and mixed. After mixing well, it was neutralized with 10% NaOH and filtered. Finally, after the product was cleaned with activated charcoal, it was dissolved with ethanol and recrystallized.

General procedure for obtaining 2-(p-substitutedphenyl)-5-[(4-substitutedphenyl)sulfonylamido] benzoxazoles (N2-N10): Target compounds was obtained by reaction of 5-amino-2-(p-substitutedphenyl)benzoxazoles with p-substituted-benzenesulfonyl chloride in the presence of dichloromethane and pyridine. Target products were crystallized from ethanol.



RESULTS & DISCUSSION

Spectral data of the compounds reveal that the target structures are obtained very purely.

Comp.	R	R'	¹ H-NMR	¹³ C-NMR	M/H	%yield	M.P.
N2	C ₆ H ₅	F	3.166-3.06 (td, 2H, J=8.0), 3.916-3.6632, 7.935 (d, H, J=8.4), 7.791-7.925 (dd, 149.16, 148.93, 148.79, 148.59, 148.45, 148.29, 148.13, 147.99, 147.84, 147.69, 147.54, 147.39, 147.24, 147.09, 146.94, 146.79, 146.64, 146.49, 146.34, 146.19, 146.04, 145.89, 145.74, 145.59, 145.44, 145.29, 145.14, 144.99, 144.84, 144.69, 144.54, 144.39, 144.24, 144.09, 143.94, 143.79, 143.64, 143.49, 143.34, 143.19, 143.04, 142.89, 142.74, 142.59, 142.44, 142.29, 142.14, 141.99, 141.84, 141.69, 141.54, 141.39, 141.24, 141.09, 140.94, 140.79, 140.64, 140.49, 140.34, 140.19, 140.04, 139.89, 139.74, 139.59, 139.44, 139.29, 139.14, 138.99, 138.84, 138.69, 138.54, 138.39, 138.24, 138.09, 137.94, 137.79, 137.64, 137.49, 137.34, 137.19, 137.04, 136.89, 136.74, 136.59, 136.44, 136.29, 136.14, 135.99, 135.84, 135.69, 135.54, 135.39, 135.24, 135.09, 134.94, 134.79, 134.64, 134.49, 134.34, 134.19, 134.04, 133.89, 133.74, 133.59, 133.44, 133.29, 133.14, 132.99, 132.84, 132.69, 132.54, 132.39, 132.24, 132.09, 131.94, 131.79, 131.64, 131.49, 131.34, 131.19, 131.04, 130.89, 130.74, 130.59, 130.44, 130.29, 130.14, 130.04, 129.89, 129.74, 129.59, 129.44, 129.29, 129.14, 128.99, 128.84, 128.69, 128.54, 128.39, 128.24, 128.09, 127.94, 127.79, 127.64, 127.49, 127.34, 127.19, 127.04, 126.89, 126.74, 126.59, 126.44, 126.29, 126.14, 125.99, 125.84, 125.69, 125.54, 125.39, 125.24, 125.09, 124.94, 124.79, 124.64, 124.49, 124.34, 124.19, 124.04, 123.89, 123.74, 123.59, 123.44, 123.29, 123.14, 122.99, 122.84, 122.69, 122.54, 122.39, 122.24, 122.09, 121.94, 121.79, 121.64, 121.49, 121.34, 121.19, 121.04, 120.89, 120.74, 120.59, 120.44, 120.29, 120.14, 120.04, 119.89, 119.74, 119.59, 119.44, 119.29, 119.14, 118.99, 118.84, 118.69, 118.54, 118.39, 118.24, 118.09, 117.94, 117.79, 117.64, 117.49, 117.34, 117.19, 117.04, 116.89, 116.74, 116.59, 116.44, 116.29, 116.14, 115.99, 115.84, 115.69, 115.54, 115.39, 115.24, 115.09, 114.94, 114.79, 114.64, 114.49, 114.34, 114.19, 114.04, 113.89, 113.74, 113.59, 113.44, 113.29, 113.14, 112.99, 112.84, 112.69, 112.54, 112.39, 112.24, 112.09, 111.94, 111.79, 111.64, 111.49, 111.34, 111.19, 111.04, 110.89, 110.74, 110.59, 110.44, 110.29, 110.14, 110.04, 109.89, 109.74, 109.59, 109.44, 109.29, 109.14, 108.99, 108.84, 108.69, 108.54, 108.39, 108.24, 108.09, 107.94, 107.79, 107.64, 107.49, 107.34, 107.19, 107.04, 106.89, 106.74, 106.59, 106.44, 106.29, 106.14, 105.99, 105.84, 105.69, 105.54, 105.39, 105.24, 105.09, 104.94, 104.79, 104.64, 104.49, 104.34, 104.19, 104.04, 103.89, 103.74, 103.59, 103.44, 103.29, 103.14, 102.99, 102.84, 102.69, 102.54, 102.39, 102.24, 102.09, 101.94, 101.79, 101.64, 101.49, 101.34, 101.19, 101.04, 100.89, 100.74, 100.59, 100.44, 100.29, 100.14, 100.04, 99.89, 99.74, 99.59, 99.44, 99.29, 99.14, 98.99, 98.84, 98.69, 98.54, 98.39, 98.24, 98.09, 97.94, 97.79, 97.64, 97.49, 97.34, 97.19, 97.04, 96.89, 96.74, 96.59, 96.44, 96.29, 96.14, 95.99, 95.84, 95.69, 95.54, 95.39, 95.24, 95.09, 94.94, 94.79, 94.64, 94.49, 94.34, 94.19, 94.04, 93.89, 93.74, 93.59, 93.44, 93.29, 93.14, 92.99, 92.84, 92.69, 92.54, 92.39, 92.24, 92.09, 91.94, 91.79, 91.64, 91.49, 91.34, 91.19, 91.04, 90.89, 90.74, 90.59, 90.44, 90.29, 90.14, 90.04, 89.89, 89.74, 89.59, 89.44, 89.29, 89.14, 88.99, 88.84, 88.69, 88.54, 88.39, 88.24, 88.09, 87.94, 87.79, 87.64, 87.49, 87.34, 87.19, 87.04, 86.89, 86.74, 86.59, 86.44, 86.29, 86.14, 85.99, 85.84, 85.69, 85.54, 85.39, 85.24, 85.09, 84.94, 84.79, 84.64, 84.49, 84.34, 84.19, 84.04, 83.89, 83.74, 83.59, 83.44, 83.29, 83.14, 82.99, 82.84, 82.69, 82.54, 82.39, 82.24, 82.09, 81.94, 81.79, 81.64, 81.49, 81.34, 81.19, 81.04, 80.89, 80.74, 80.59, 80.44, 80.29, 80.14, 80.04, 79.89, 79.74, 79.59, 79.44, 79.29, 79.14, 78.99, 78.84, 78.69, 78.54, 78.39, 78.24, 78.09, 77.94, 77.79, 77.64, 77.49, 77.34, 77.19, 77.04, 76.89, 76.74, 76.59, 76.44, 76.29, 76.14, 75.99, 75.84, 75.69, 75.54, 75.39, 75.24, 75.09, 74.94, 74.79, 74.64, 74.49, 74.34, 74.19, 74.04, 73.89, 73.74, 73.59, 73.44, 73.29, 73.14, 72.99, 72.84, 72.69, 72.54, 72.39, 72.24, 72.09, 71.94, 71.79, 71.64, 71.49, 71.34, 71.19, 71.04, 70.89, 70.74, 70.59, 70.44, 70.29, 70.14, 70.04, 69.89, 69.74, 69.59, 69.44, 69.29, 69.14, 68.99, 68.84, 68.69, 68.54, 68.39, 68.24, 68.09, 67.94, 67.79, 67.64, 67.49, 67.34, 67.19, 67.04, 66.89, 66.74, 66.59, 66.44, 66.29, 66.14, 65.99, 65.84, 65.69, 65.54, 65.39, 65.24, 65.09, 64.94, 64.79, 64.64, 64.49, 64.34, 64.19, 64.04, 63.89, 63.74, 63.59, 63.44, 63.29, 63.14, 62.99, 62.84, 62.69, 62.54, 62.39, 62.24, 62.09, 61.94, 61.79, 61.64, 61.49, 61.34, 61.19, 61.04, 60.89, 60.74, 60.59, 60.44, 60.29, 60.14, 60.04, 59.89, 59.74, 59.59, 59.44, 59.29, 59.14, 58.99, 58.84, 58.69, 58.54, 58.39, 58.24, 58.09, 57.94, 57.79, 57.64, 57.49, 57.34, 57.19, 57.04, 56.89, 56.74, 56.59, 56.44, 56.29, 56.14, 55.99, 55.84, 55.69, 55.54, 55.39, 55.24, 55.09, 54.94, 54.79, 54.64, 54.49, 54.34, 54.19, 54.04, 53.89, 53.74, 53.59, 53.44, 53.29, 53.14, 52.99, 52.84, 52.69, 52.54, 52.39, 52.24, 52.09, 51.94, 51.79, 51.64, 51.49, 51.34, 51.19, 51.04, 50.89, 50.74, 50.59, 50.44, 50.29, 50.14, 50.04, 49.89, 49.74, 49.59, 49.44, 49.29, 49.14, 48.99, 48.84, 48.69, 48.54, 48.39, 48.24, 48.09, 47.94, 47.79, 47.64, 47.49, 47.34, 47.19, 47.04, 46.89, 46.74, 46.59, 46.44, 46.29, 46.14, 45.99, 45.84, 45.69, 45.54, 45.39, 45.24, 45.09, 44.94, 44.79, 44.64, 44.49, 44.34, 44.19, 44.04, 43.89, 43.74, 43.59, 43.44, 43.29, 43.14, 42.99, 42.84, 42.69, 42.54, 42.39, 42.24, 42.09, 41.94, 41.79, 41.64, 41.49, 41.34, 41.19, 41.04, 40.89, 40.74, 40.59, 40.44, 40.29, 40.14, 40.04, 39.89, 39.74, 39.59, 39.44, 39.29, 39.14, 38.99, 38.84, 38.69, 38.54, 38.39, 38.24, 38.09, 37.94, 37.79, 37.64, 37.49, 37.34, 37.19, 37.04, 36.89, 36.74, 36.59, 36.44, 36.29, 36.14, 35.99, 35.84, 35.69, 35.54, 35.39, 35.24, 35.09, 34.94, 34.79, 34.64, 34.49, 34.34, 34.19, 34.04, 33.89, 33.74, 33.59, 33.44, 33.29, 33.14, 32.99, 32.84, 32.69, 32.54, 32.39, 32.24, 32.09, 31.94, 31.79, 31.64, 31.49, 31.34, 31.19, 31.04, 30.89, 30.74, 30.59, 30.44, 30.29, 30.14, 30.04, 29.89, 29.74, 29.59, 29.44, 29.29, 29.14, 28.99, 28.84, 28.69, 28.54, 28.39, 28.24, 28.09, 27.94, 27.79, 27.64, 27.49, 27.34, 27.19, 27.04, 26.89, 26.74, 26.59, 26.44, 26.29, 26.14, 25.99, 25.84, 25.69, 25.54, 25.39, 25.24, 25.09, 24.94, 24.79, 24.64, 24.49, 24.34, 24.19, 24.04, 23.89, 23.74, 23.59, 23.44, 23.29, 23.14, 22.99, 22.84, 22.69, 22.54, 22.39, 22.24, 22.09, 21.94, 21.79, 21.64, 21.49, 21.34, 21.19, 21.04, 20.89, 20.74, 20.59, 20.44, 20.29, 20.14, 20.04, 19.89, 19.74, 19.59, 19.44, 19.29, 19.14, 18.99, 18.84, 18.69, 18.54, 18.39, 18.24, 18.09, 17.94, 17.79, 17.64, 17.49, 17.34, 17.19, 17.04, 16.89, 16.74, 16.59, 16.44, 16.29, 16.14, 15.99, 15.84, 15.69, 15.54, 15.39, 15.24, 15.09, 14.94, 14.79, 14.64, 14.49, 14.34, 14.19, 14.04, 13.89, 13.74, 13.59, 13.44, 13.29, 13.14, 12.99, 12.84, 12.69, 12.54, 12.39, 12.24, 12.09, 11.94, 11.79, 11.64, 11.49, 11.34, 11.19, 11.04, 10.89, 10.74, 10.59, 10.44, 10.29, 10.14, 10.04, 9.89, 9.74, 9.59, 9.44, 9.29, 9.14, 8.99, 8.84, 8.69, 8.54, 8.39, 8.24, 8.09, 7.94, 7.79, 7.64, 7.49, 7.34, 7.19, 7.04, 6.89, 6.74, 6.59, 6.44, 6.29, 6.14, 5.99, 5.84, 5.69, 5.54, 5.39, 5.24, 5.09, 4.94, 4.79, 4.64, 4.49, 4.34, 4.19, 4.04, 3.89, 3.74, 3.59, 3.44, 3.29, 3.14, 2.99, 2.84, 2.69, 2.54, 2.39, 2.24, 2.09, 1.94, 1.79, 1.64, 1.49, 1.34, 1.19, 1.04, 0.89, 0.74, 0.59, 0.44, 0.29, 0.14, 0.04, -0.11, -0.26, -0.41, -0.56, -0.71, -0.86, -1.01, -1.16, -1.31, -1.46, -1.61, -1.76, -1.91, -2.06, -2.21, -2.36, -2.51, -2.66, -2.81, -2.96, -3.11, -3.26, -3.41, -3.56, -3.71, -3.86, -4.01, -4.16, -4.31, -4.46, -4.61, -4.76, -4.91, -5.06, -5.21, -5.36, -5.51, -5.66, -5.81, -5.96, -6.11, -6.26, -6.41, -6.56, -6.71, -6.86, -7.01, -7.16, -7.31, -7.46, -7.61, -7.76, -7.91, -8.06, -8.21, -8.36, -8.51, -8.66, -8.81, -8.96, -9.11, -9.26, -9.41, -9.56, -9.71, -9.86, -10.01, -10.16, -10.31, -10.46, -10.61, -10.76, -10.91, -11.06, -11.21, -11.36, -11.51, -11.66, -11.81, -11.96, -12.11, -12.26, -12.41, -12.56, -12.71, -12.86, -13.01, -13.16, -13.31, -13.46, -13.61, -13.76, -13.91, -14.06, -14.21, -14.36, -14.51, -14.66, -14.81, -14.96, -15.11, -15.26, -15.41, -15.56, -15.71, -15.86, -16.01, -16.16, -16.31, -16.46, -16.61, -16.76, -16.91, -17.06, -17.21, -17.36, -17.51, -17.66, -17.81, -17.96, -18.11, -18.26, -18.41, -18.56, -18.71, -18.86, -19.01, -19.16, -19.31, -19.46, -19.61, -19.76, -19.91, -20.06, -20.21, -20.36, -20.51, -20.66, -20.81, -20.96, -21.11, -21.26, -21.41, -21.56, -21.71, -21.86, -22.01, -22.16, -22.31, -22.46, -22.61, -22.76, -22.91, -23.06, -23.21, -23.36, -23.51, -23.66, -23.81, -23.96, -24.11, -24.26, -24.41, -24.56, -24.71, -24.86, -25.01, -25.16, -25.31, -25.46, -25.61, -25.76, -25.91, -26.06, -26.21, -26.36, -26.51, -26.66, -26.81, -26.96, -27.11, -27.26, -27.41, -27.56, -27.71, -27.86, -28.01, -28.16, -28.31, -28.46, -28.61, -28.76, -28.91, -29.06, -29.21, -29.36, -29.51, -29.66, -29.81, -29.96, -30.11, -30.26, -30.41, -30.56, -30.71, -30.86, -31.01, -31.16, -31.31, -31.46, -31.61, -31.76, -31.91, -32.06, -32.21, -32.36, -32.51, -32.66, -32.81, -32.96, -33.11, -33.26, -33.41, -33.56, -33.71, -33.86, -34.01, -34.16, -34.31, -34.46, -34.61, -34.76, -34.91, -35.06, -35.21, -35.36, -35.51, -35.66, -35.81, -35.96, -36.11, -36.26, -36.41, -36.56, -36.71, -36.86, -37.01, -37.16, -37.31, -37.46, -37.61, -37.76, -37.91, -38.06, -38.21, -38.36, -38.51, -38.66, -38.81, -38.96, -39.11, -39.26, -39.41, -39.56, -39.71, -39.86, -40.01, -40.16, -40.31, -40.46, -40.61, -40.76, -40.91, -41.06, -41.21, -41.36, -41.51, -41.66, -41.81, -41.96, -42.11, -42.26, -42.41, -42.56, -42.71, -42.86, -43.01, -43.16, -43.31, -43.46, -43.61, -43.76, -43.91, -44.06, -44.21, -44.36, -44.51, -44.66, -44.81, -44.96, -45.11, -45.26, -45.41, -45.56, -45.71, -45.86, -46.01, -46.16, -46.31, -46.46, -46.61, -46.76, -46.91, -47.06, -47.21, -47.36, -47.51, -47.66, -47.81, -47.96, -48.11, -48.26, -48.41, -48.56, -48.71, -48.86, -49.01, -49.16, -49.31, -49.46, -49.61, -49.76, -49.91, -50.06, -50.21, -50.36, -50.51, -50.66, -50.81, -50.96, -51.11, -51.26, -51.41, -51.56, -51.71, -51.86, -52.01, -52.16, -52.31, -52.46, -52.61, -52.76, -52.91, -53.06, -53.21, -53.36, -53.51, -53.66, -53.81, -53.96, -54.11, -54.26, -54.41, -54.56, -54.71, -54.86, -55.01, -55.16, -55.31, -55.46, -55.61, -55.76, -55.91, -56.06, -56.21, -56.36, -56.51, -56.66, -56.81, -56.96, -57.11, -57.26, -57.41, -57.56, -57.71, -57.86, -58.01, -58.16, -58.31, -58.46, -58.61, -58.76, -58.91, -59.06, -59.21, -59.36, -59.51, -59.66, -59.81, -59.96, -60.11, -60.26, -60.41, -60.56, -60.71, -60.86, -61.01, -61.16, -61.31, -61.46, -61.61, -61.76, -61.91, -62.06, -62.21, -62.36, -62.51, -62.66, -62.81, -62.96, -63.11, -63.26, -63.41, -63.56, -63.71, -63.86, -64.01, -64.16, -64.31, -64.46, -64.61, -64.76, -64.91, -65.06, -65.21, -65.36, -65.51, -65.66, -65.81, -65.96, -66.11, -66.26, -66.41, -66.56, -66.71, -66.86, -67.01, -67.16, -67.31, -67.46, -67.61, -67.76, -67.91, -68.06, -68.21, -68.36, -68.51, -68.66, -68.81, -68.96, -69.11, -69.26, -69.41, -69.56, -69.71, -69.86, -70.01, -70.16, -70.31, -70.46, -70.61, -70.76, -70.91, -71.06, -71.21, -71.36, -71.51, -71.66, -71.81, -71.96, -72.11, -72.26, -72.41, -72.56, -72.71, -72.86, -73.01, -73.16, -73.31, -73.46, -73.61, -73.76, -73.91, -74.06, -74.21, -74.36, -74.51, -74.66, -74.81, -74.96, -75.11, -75.26, -75.41, -75.56, -75.71, -75.86, -76.01, -76.16, -76.31, -76.46, -76.61, -76.76, -76.91, -77.06, -77.21, -77.36, -77.51, -77.66, -77.81, -77.96, -78.11, -78.26, -78.41, -78.56, -78.71, -78.86, -79.01, -79.16, -79.31, -79.46, -79.61, -79.76, -79.91, -80.06, -80.21, -80.36, -80.51, -80.66, -80.81, -80.96, -81.11, -81.26, -81.41, -81.56, -81.71, -81.86, -82.01, -82.16, -82.31, -82.46, -82.61, -82.76, -82.91, -83.06, -83.21, -83.36, -83.51, -83.66, -83.81, -83.96, -84.11, -84.26, -84.41, -84.56, -84.71, -84.86, -85.01, -85.16, -85.31, -85.46, -85.61, -85.76, -85.91, -86.06, -86.21, -86.36, -86.51, -86.66, -86.81, -86.96, -87.11, -87.26, -87.41, -87.56, -87.71, -87.86, -88.01, -88.16, -88.31, -88.46, -88.61, -88.76, -88.91, -89.06, -89.21, -89.36, -89.51, -89.66, -89.81, -89.96, -90.11, -90.26, -90.41, -90.56, -90.71, -90.86, -91.01, -91.16, -91.31, -91.46, -91.61, -91.76, -91.91, -92.06, -92.21, -92.36, -92.51, -92.66, -92.81, -92.96, -93.11, -93.26, -93.41, -93.56, -93.71, -93.86, -94.01, -94.16, -94.31, -94.46, -94.61, -94.76, -94.91, -95.06, -95.21, -95.36, -95.51, -95.66, -95.81, -95.96, -96.11, -96.26, -96.41, -96.56, -96.71, -96.86, -97.01, -97.16, -97.31, -97.46, -97.61, -97.76, -97.91, -98.06, -98.21, -98.36, -98.51, -98.66, -98.81, -98.96, -99.11, -99.26, -99.41, -99.56, -99.71, -99.86, -100.01, -100.16, -100.31, -100.46, -100.61, -100.76, -100.91, -101.06, -101.21, -101.36, -101.51, -101.66, -101.81, -101.96, -102.11, -102.26, -102.41, -102.56, -102.71, -102.86, -103.01, -103.16, -103.31, -103.46, -103.61, -103.76, -103.91, -104.06, -104.21, -104.36, -104.51, -104.66, -104.81, -104.96, -105.11, -105.26, -105.41, -105.56, -105.71, -105.86, -106.01, -106.16, -106.31, -106.46, -106.61, -106				



SYNTHESIS OF SOME NOVEL SCHIFF BASES INCORPORATED WITH INDAZOLE MOIETY

¹Kayikci-Pasa, N., ¹Gurkan-Alp, AS.

¹Ankara University, Faculty of Pharmacy, Department of Pharmaceutical Chemistry, Ankara, Turkey

salp@ankara.edu.tr



Introduction

Since cancer is currently one of the leading causes of death in many countries, new compounds that could affect the molecular mechanisms of cancer need to be designed and synthesized. Indazole unit is an important heterocyclic structure and indazole derivatives exhibit a wide range of bioactivity, including anticancer, antidiabetic, analgesic, antiinflammatory, antidepressant, anti-HIV, anti-platelet, and serotonin 5-HT₃ receptor antagonist activity (1-3). Indazoles fused with the aromatic ring at the 1st and 2nd position are well known for their antihypertensive and anticancer properties (2). Indazole-containing drugs axitinib, pazopanib, and linafinib were approved for clinical use based on their anticancer effects (3) (Figure 1). In this study, we aimed to synthesize a number of novel Schiff base derivatives incorporated with indazole moiety.

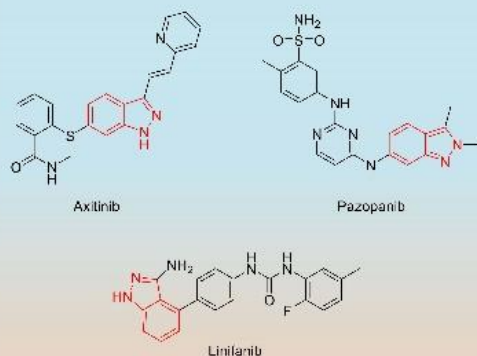


Figure 1. Some indazole-containing anticancer drugs.

Materials and Methods

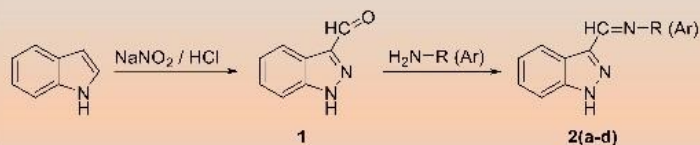
All starting materials, reagents and solvents were high-grade commercial products purchased from Sigma-Aldrich or Merck. The structures of all synthesized compounds were assigned on the basis of ¹H-NMR and Mass spectral analyses. Analytical thin-layer chromatographies (TLC) were run on silica gel 60 F₂₅₄ plates (Merck, Germany). Column chromatographies were accomplished on silica gel 60 (40-63 µm particle size) (Merck, Germany). ¹H-NMR spectra were recorded employing a Varian Mercury 400 MHz FT spectrometer (Varian, Palo Alto, CA, USA) in CDCl₃. Chemical shifts (δ) are given in ppm relative to tetramethylsilane, and coupling constants (J) are reported in Hz. Mass spectra were recorded on a Waters Micromass ZQ (Micromass UK, Manchester, UK) in the positive-ion mode in a Waters Alliance instrument. ¹H-NMR and Mass analyses were performed at The Central Instrumentation Laboratory of the Pharmacy Faculty of Ankara University, Ankara, Turkey.

Synthesis of indazole-3-carbaldehyde 1

To a solution of NaNO₂ (8 mmol) in water (4 ml) and DMF (3 ml) at 0°C was added slowly HCl (aq.) (1.33 ml of 2 N). A solution of indole (1 mmol) in DMF (3 ml) was then added at 0°C over a period of 2 h using a syringe pump. After addition, the reaction was stirred 3 h at room temperature. The product was purified by column chromatography on silica gel, eluting with petroleum ether / EtOAc (4 : 1) to give the pure compound (4, 5).

Synthesis of 1-(1H-indazol-3-yl)-N-substituted-methanimino derivatives 2(a-d)

1H-indazole-3-carbaldehyde (0.65 mmol) was added to ethanol suspension of appropriate amine (0.47 mmol) and the mixture was stirred at reflux temperature. The reaction was monitored with TLC. After the reaction was completed, the solvent was evaporated under vacuum. Resulting crude was purified with silicagel column chromatography using dichloromethane / methanol solvent system (6).



Scheme 1. Synthetic route of the targeted compounds.

Results and Discussion

Indazole-3-carbaldehyde was synthesized from indole in the presence of HCl (aq.) and NaNO₂. Then, final Schiff bases 1-(1H-indazol-3-yl)-N-substituted-methanimine derivatives 2(a-d) were prepared in methanol by using the aldehyde and appropriate benzimidazole / benzothiazole derived amines (Scheme 1, Table 1). All of the compounds were purified with silicagel column chromatography and obtained with low yield. Structural elucidation of the targeted compounds were performed with LC-MS and NMR analysis. Spectral data are compatible with the desired structure.

Indazole-3-carbaldehyde 1

Yellow solid (Yield 40%). MS (ESI+) *m/z* (rel. intensity): 147 (M+H, 100). ¹H NMR δ (400 MHz, DMSO-*d*₆): 14.172 (s, 1H, -CHO), 10.175 (s, 1H, -NH), 8.11 (d, 1H, J = 8.4 Hz), 7.68 (d, 1H, J = 8.4 Hz), 7.47 (t, 1H, J = 7.6 Hz), 7.34 (t, 1H, J = 7.6 Hz).

In the NMR spectra of the targeted imine derivatives, proton signals belonging to aromatic hydrogens were observed in 7.14-8.48 ppm. Imino hydrogen (CH=N), methylene protons (CH₂CO), and NH displayed 1 singlet signal.

Table 1. Mass spectra (ESI+) of the synthesized compounds

Compound	R (Ar)	MS (ESI+) <i>m/z</i> (rel. intensity)
2a		262 (M+H, 100)
2b		276 (M+H, 100)
2c		279 (M+H, 100)
2d		293 (M+H, 100)

Conclusions

In this study, novel 1-(1H-indazol-3-yl)-N-substituted-methanimines were prepared and their characterization were performed. Researches will be conducted to reveal their cytotoxic effects and mechanisms of their actions on cell viability.

References

- Li P et al. (2012). Synthesis of Substituted 1H-Indazoles from Arynes and Hydrazones, *J. Org. Chem.*, 77: 3149-3158.
- Gulwadi DD et al. (2015). Synthesis of indazole motifs and their medicinal importance: an overview, *Eur. J. Med. Chem.*, 90: 737-731.
- Wang XR et al. (2021). Design, synthesis and biological evaluation of novel 2-(4-(1H-indazol-3-yl)-1H-pyrazol-1-yl)acetamide derivatives as potent VEGFR 2 inhibitors, *Eur. J. Med. Chem.*, 213: 113192.
- Chevalier A et al. (2018). An optimized procedure for direct access to 1H-indazole-3-carboxaldehyde derivatives by nitrosation of indoles, *RSC Adv.*, 8: 13721.
- See CS et al. (2018). Discovery of the cancer cell selective dual acting anti-cancer agent (Z)-2-(1H-indol-3-yl)-3-(isoquinolin-5-yl)acrylonitrile (A131), *Eur. J. Med. Chem.*, 156: 344-367.
- Wang H et al. (2020). A new fluorescent probe based on imidazole[2,1-b]benzothiazole for sensitive and selective detection of Cu²⁺, *Journal of Molecular Structure*, 1203: 127354.



SYNTHESIS OF SOME NOVEL *N'*-((ARYL)METHYLENE)-1H-INDOLE-5-CARBOHYDRAZIDES

¹Gurkan-Alp, AS., ¹Avuka, OF.

¹ Ankara University, Faculty of Pharmacy, Department of Pharmaceutical Chemistry, Ankara, Turkey

salp@ankara.edu.tr



Introduction

Indole ring is considered as an important core of some natural and synthetic molecules with different biological activities. These bioactive molecules are known to prevent proliferation of different cancer cells. Although anticarcinogenic and anti-metastatic effectiveness of indole derivatives were reported in many studies, it needs to be described more potent and selective cytotoxic agents (1, 2).

On the other hand, as a special member of Schiff bases, hydrazones and their derivatives are molecules of interest in medicinal chemistry due to their wide variety of biological activities (3). It was reported in many studies that hydrazone-derived compounds displayed antibacterial, antifungal, antiviral, antineoplastic, antiprotozoal, antihelminthic, anticonvulsant, antidepressant, antioxidant, antiplatelet, analgesic and anti-inflammatory activities. Thanks to their diverse biological and clinical applications, they are very important for development of potential new drugs.

In this study, we aimed to synthesize a number of novel hydrazone derivatives incorporated with indole core. Their structural elucidations were performed. Anticancer activity studies of these compounds will be conducted.

Materials and Methods

All starting materials, reagents and solvents were high-grade commercial products purchased from Sigma-Aldrich or Merck. The structures of all synthesized compounds were assigned on the basis of ¹H-NMR and Mass spectral analyses. Analytical thin-layer chromatographies (TLC) were run on silica gel 60 F₂₅₄ plates (Merck, Germany). Column chromatographies were accomplished on silica gel 60 (40-63 µm particle size) (Merck, Germany). ¹H-NMR spectra were recorded employing a Varian Mercury 400 MHz FT spectrometer (Varian, Palo Alto, CA, USA) in CDCl₃. Chemical shifts (δ) are given in ppm relative to tetramethylsilane, and coupling constants (*J*) are reported in Hz. Mass spectra were recorded on a Waters Micromass ZQ (Micromass UK, Manchester, UK) in the positive-ion mode in a Waters Alliance instrument. ¹H-NMR and Mass analyses were performed at The Central Instrumentation Laboratory of the Pharmacy Faculty of Ankara University, Ankara, Turkey.

Synthesis of methyl 1H-indole-5-carboxylate **2**

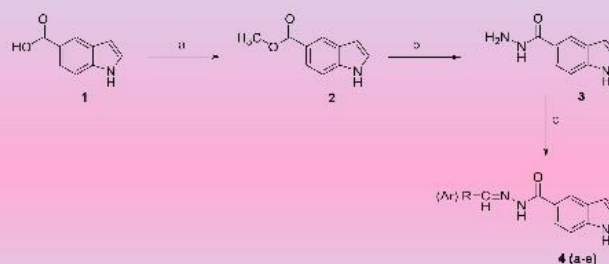
1H Indole 5 carboxylic acid (1 g, 6.2 mmol) was added potassium carbonate (0.9 g, 6.5 mmol) and methyl iodide (1.14 g, 8 mmol) in *N,N*-Dimethylformamide (5 ml). Reaction mixture was stirred for 4 hours at room temperature and then added water to quench the reaction. The obtained light pink solid was filtered, dried, and used for the following step (4, 5).

Synthesis of 1H-Indole-5-carbohydrazide **3**

1H-Indole-5-carbohydrazide was synthesized by reacting methyl 1H-indole-5-carboxylate (1 mmol) with hydrazine hydrate (10 mmol). The reaction was performed in the presence of abs. ethanol (5 ml) as the solvent and refluxed for 10 h at 85-90°C. The reaction mixture was checked for completion using TLC. After the reaction completed, ethanol was removed by vacuum and residue collected was rinsed with ice-cold water. Light yellow product was collected by filtration and was purified with silicagel column chromatography (6).

Synthesis of *N'*-((aryl)methylene)-1H-indole-5-carbohydrazides **4(a-e)**

1H-Indole-5-carbohydrazide (1 mmol) in methanol (15 ml) was allowed to react with appropriate aldehydes (1.1 mmol) in the presence of acetic acid (2 drops) as catalyst. The reaction was refluxed for 6 h. The reaction mixture was checked for completion using TLC. After completion, the reaction mixture was rotavaped and residue collected was rinsed with water. Crude product was purified with column chromatography using dichloromethane / methanol (100:5) solvent system (6).



Scheme 1. Synthetic route of the targeted compounds. a. DMF, NaHCO₃, CH₃I, r.t. b. NH₂NH₂·H₂O, abs. ethanol, reflux. c. Appropriate aldehydes, methanol, reflux.

Results and Discussion

Methyl-1H-indole-5-carboxylate was prepared from 1H-indole-5-carboxylic acid in dimethylformamide in the presence of sodium bicarbonate and iodomethane. A mixture of crude ester and hydrazine hydrate in ethanol was heated at reflux to give 1H-indole-5-carbohydrazide (4, 5). Then, final hydrazones *N'*-((aryl)methylene)-1H-indole-5-carbohydrazides were derived from the hydrazone compound and appropriate aldehydes according to the process described in literature (6) (Scheme 1, Table 1). 1H-Indole-5-carbohydrazide and all of the targeted hydrazones were purified with silicagel column chromatography. Structural elucidation of the targeted hydrazones were performed with LC-MS, NMR, and elemental analysis. The spectral details are in accordance with the final compounds.

In the ¹H-NMR spectra of the targeted hydrazone derivatives, proton signals belonging to aromatic hydrogens were observed in 7.40-8.45 ppm. Imino hydrogen was observed in 6.56-6.61 ppm. Indol NH and hydrazone NH were observed in 11.40-11.89 ppm. Imino hydrogen (CH=N) and NH displayed 1 singlet signal.

Table 1. Mass spectra (ESI+) of the synthesized compounds.

Compound	R (Ar)	MS (ESI+) <i>m/z</i> (rel. intensity)
4a	Phenyl-	264 (M+H, 100)
4b	1-Naphtyl-	314 (M+H, 100)
4c	2-Naphtyl-	314 (M+H, 100)
4d	2-Hydroxy-1-naphtyl-	330 (M+H, 100)
4e	4-Pyridyl-	265 (M+H, 100)

Conclusions

In this study, novel *N'*-((aryl)methylene)-1H-indole-5-carbohydrazide derivatives were prepared and their characterization were performed. Studies need to be conducted to determine their effects on different cancer cell lines.

References

1. Sachdeva H et al. (2020). J. Chil. Chem. Soc., 65(3): 4900-4907.
2. Sidhu SJ et al. (2016). Anti Cancer Agents Med. Chem., 16(2): 160-173.
3. Brum JOC et al. (2020). Mini Reviews in Medicinal Chemistry, 20(5): 347-368.
4. Binti YU et al. (2017). WO2017/143291.
5. Rao SY et al. (2018). World J. Pharm. Res., 7(6): 877-882.
6. Nozari T et al. (2017). Bioorganic Chemistry, 72: 248-265.



SYNTHESIS OF SOME NOVEL 4-(1H-BENZIMIDAZOL-1-YL)-N'-BENZYLIDENEBENZOHYDRAZIDE DERIVATIVES

Alp, M., Alp, AS.

Ankara University, Faculty of Pharmacy, Department of Pharmaceutical Chemistry, Ankara, Turkey,
malp@ankara.edu.tr



Introduction

Benzimidazole is an essential pharmacophore with wide anticancer potential. Benzimidazole-containing anticancer compounds have selective potential that depends on the substitution of the benzimidazole nucleus (1). The platelet-derived growth factor (PDGF) plays a vital role as a regulator of cell growth. Promising platelet derived growth factor receptor (PDGFR) inhibitor activity of some 1-phenyl benzimidazoles have been reported (Figure 1) (2,3).

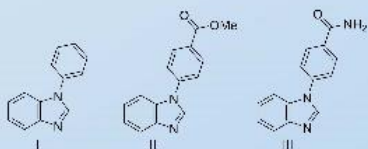


Figure 1. Some 1-phenyl benzimidazoles as PDGFR inhibitors.

In this study, we aimed to synthesize some novel 4-(1H-benzimidazol-1-yl)-N'-benzylidenbenzohydrazide derivatives. Their characterizations were performed. Anticancer activity studies of the synthesized compounds are currently in progress.

Materials and Methods

All starting materials, reagents and solvents were high grade commercial products purchased from Sigma-Aldrich or Merck. ¹H-NMR and ¹³C-NMR spectra were recorded employing a Varian Mercury 400 MHz FT-NMR spectrometer. Mass spectra were taken on a Waters Micromass ZQ connected with a Waters Alliance HPLC, using the ESI(+) method. Elemental analyses were performed using a Leco CHNS-932. All instrumental analysis results of the synthesized compounds were found to be consistent with their chemical structure.

Synthesis of 1H-Benzimidazole 1

o-Phenylenediamine (10 mmol) and formic acid (11 mmol) mixture was allowed to reflux for 8 h. After the reaction mixture was cooled to room temperature, 5N NaOH (aq.) was added. The precipitate was filtered and rinsed with water. 1H-Benzimidazole 1 was obtained by recrystallization from water (4).

Synthesis of 4-benzimidazole-1-yl-benzoic acid 2

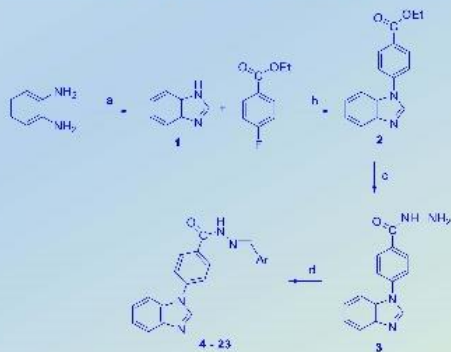
The mixture of benzimidazole (1.1 mmol), ethyl-4-fluorobenzoate (1 mmol) and K₂CO₃ (1.5 mmol) in DMF (10 ml) were heated at 100°C for 48 h. After the solvent was removed under vacuum, the residue was rinsed with water and extracted with ethyl acetate. Removal of the solvent gave a crude product that was recrystallized from methanol to obtain 2 (5).

Synthesis of 4-(1H-benzimidazole-1-yl)benzoic acid hydrazide 3

4-(1H-Benzimidazole-1-yl)benzoic acid hydrazide 3 was synthesized by reacting ethyl 4-(1H-benzimidazol-1-yl)benzoate 2 (1 mmol) with hydrazine hydrate (10 mmol) according to the known procedure. The reaction was performed in the presence of abs. ethanol (5 ml) and refluxed for 6 h. After the reaction completed, solvent was removed by vacuum and residue collected was rinsed with ice-cold water. White solid was collected by filtration and purified with recrystallization from ethanol.

Synthesis of 4-(1H-benzimidazol-1-yl)-N'-benzylidenbenzohydrazides 4-23

A known procedure was used to obtain the final compounds. 4-(1H-benzimidazole-1-yl)benzoic acid hydrazide 3 (1 mmol) in ethanol (15 ml) was allowed to react with appropriate aldehydes (1.1 mmol). The reaction was refluxed for 3 h. Then the solvent was evaporated and residue was rinsed with water. Crude product was purified with recrystallization from methanol.



Scheme 1. Synthetic route of the synthesized compounds. (a) HCOOH; (b) DMF, anh. K₂CO₃; (c) N₂H₄·H₂O, MeOH; (d) corresponding aldehydes, EtOH.

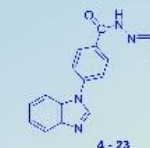
Results and Discussion

1H-Benzimidazole ring was built by cyclization of the *o*-phenylenediamine and formic acid (4). Then, reaction of the 1H-benzimidazole 1 with ethyl 4-fluorobenzoate in DMF in the presence of anhydrous K₂CO₃ gave ethyl 4-(1H-benzimidazol-1-yl)benzoate 2 (5). This compound was treated with excess of hydrazine hydrate to obtain 4-(1H-benzimidazole-1-yl)benzoic acid hydrazide 3. At final step, reaction of the hydrazide derivative with corresponding substituted benzaldehydes gave the final products 4-23 (Scheme 1, Table 1).

Structural elucidation of the targeted hydrazones were performed with LC MS, NMR, and elemental analysis. The spectral details are in accordance with the final compounds.

In the ¹H-NMR spectra of the targeted hydrazone derivatives, proton signals belonging to aromatic hydrogens were observed in 7.01–9.53 ppm. Imino hydrogen (CH=N) was observed in 8.41–9.16 ppm. Hydrazone NH were observed in 11.84–12.37 ppm. Imino hydrogen (CH=N) and NH displayed 1 singlet signal.

Table 1. Mass spectra (ESI+) of the synthesized compounds.



	Ar	Molecular Formula	MS (ESI+) m/z (rel. intensity)
4	Phenyl	C ₂₀ H ₁₃ N ₂ O	341(M+H, 100)
5	4-Fluorophenyl	C ₂₀ H ₁₃ FN ₂ O	359(M+H, 100)
6	4-Chlorophenyl	C ₂₁ H ₁₂ ClN ₂ O	375(M+H, 100)
7	2,4-Dichlorophenyl	C ₂₀ H ₁₀ Cl ₂ N ₂ O	377(M+H+2, 33) 409(M+H, 100) 411(M+H-2, 62) 413(M+H+2, 2, 22)
8	3,4-Dichlorophenyl	C ₂₀ H ₁₀ Cl ₂ N ₂ O	409(M+H, 100) 411(M+H-2, 62) 413(M+H+2, 2, 22)
9	4-Chloro-3-fluorophenyl	C ₂₀ H ₁₀ ClFN ₂ O	385(M+H, 100) 395(M+H+2, 33)
10	4-Chloro-3-nitrophenyl	C ₂₀ H ₁₀ ClN ₂ O ₃	420(M+H, 100) 422(M+H+2, 33)
11	2-Nitrophenyl	C ₂₁ H ₁₄ N ₂ O ₃	366(M+H, 100)
12	3-Cyanophenyl	C ₂₀ H ₁₂ N ₂ O	366(M+H, 100)
13	4-Cyanophenyl	C ₂₀ H ₁₂ N ₂ O	366(M+H, 100)
14	2-Carboxyphenyl	C ₂₁ H ₁₄ N ₂ O ₃	366(M+H, 100)
15	3-Carboxyphenyl	C ₂₁ H ₁₄ N ₂ O ₃	366(M+H, 100)
16	4-Carboxyphenyl	C ₂₁ H ₁₄ N ₂ O ₃	366(M+H, 100)
17	4-Ethoxyphenyl	C ₂₂ H ₁₆ N ₂ O ₂	366(M+H, 100)
18	3,4-Dimethoxyphenyl	C ₂₂ H ₁₆ N ₂ O ₃	401(M+H, 100)
19	4-Benzyloxyphenyl	C ₂₅ H ₂₀ N ₂ O ₂	447(M+H, 100)
20	3,4-Dibenzoyloxyphenyl	C ₂₈ H ₂₄ N ₂ O ₄	553(M+H, 100)
21	Naphthalen-1-yl	C ₂₀ H ₁₂ N ₂ O	391(M+H, 100)
22	2-Hydroxynaphthalen-1-yl	C ₂₀ H ₁₂ N ₂ O ₂	407(M+H, 100)
23	Naphthalen-2-yl	C ₂₀ H ₁₂ N ₂ O	391(M+H, 100)

References

1. Siddhar-Goud N., Kumar P. et al. (2020). In: Varadachariar BP (ed). Heterocycles – Synthesis and Biological Activities. IntechOpen Ltd., UK.
2. Palmer DD, Smith JZ et al. (1998). Journal of Medicinal Chemistry, 41: 5457-5465
3. Okamoto M, Sa to K et al. (2011). Bioorganic & Medicinal Chemistry, 12: 486-483.
4. Furniss JS, Hannaford AJ et al. (1985). Vogel's Textbook of Practical Organic Chemistry. Longman Scientific and Technical, UK, pp 1162-1153.
5. Aljor, A, Lame P et al. (2010). New Journal of Chemistry, 34: 2502-2514.

DETERMINATION OF NOVEL UREA AND SULFONAMIDE DERIVATIVES OF ISATIN SCHIFF BASES AS POTENTIAL RECEPTOR TYROSINE KINASE INHIBITOR BY MOLECULAR DOCKING STUDIES

¹Demirel, UU., ²Ölgen, S.

¹ Altınbaş University, Pharmaceutical Chemistry, Istanbul, Turkey, ural.demirel@altinbas.edu.tr

² Biruni University, Department of Pharmaceutical Chemistry, İstanbul, Turkey, solgen@biruni.edu.tr

Introduction: In this study, we have reported the in-silico studies of novel potential active compounds by designing new, urea and sulfonamide derivatives of isatin Schiff bases. These compounds were created by taken into consideration from known active similar structures like urea containing **sorafenib** and benzylidene containing **sunitinib** (1). The enzyme-receptor interactions of compounds on VEGFR2 (PDB ID for 4AGD) were studied compared to the reference compound **sunitinib**.

Materials and Methods: The crystal structures of the receptor protein-tyrosine kinase of VEGFR2 were obtained from the Protein Data bank (PDB, <http://www.rcsb.org>). The docking study was performed in Auto Dock vina 4.2.6 software and the 3D compound-protein docking possess were analyzed by using Pymol 4.2.6.

Comp.	Energy Score (kcal mol ⁻¹) ^a	RMSD Value ^b	H-bond (distance Å) ^c
2b	-14.57	0.31	a with 1 H of CYS919 (1.786)
sunitinib	-12.27	0.5	a with 1 H of CYS919 (1.682) b with 1 O of GLU917 (1.917)

^a Lowest energy values show better interaction with receptor active site.

^b Lowest RMSD values show the closeness of compounds to active site

^c Distance of hydrogen bonds of amino acids

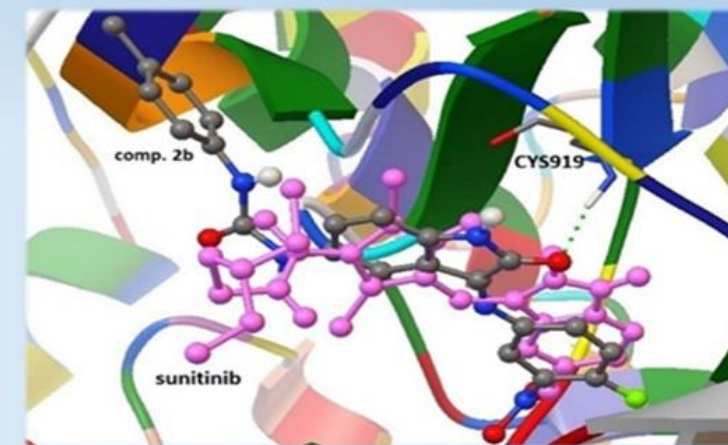
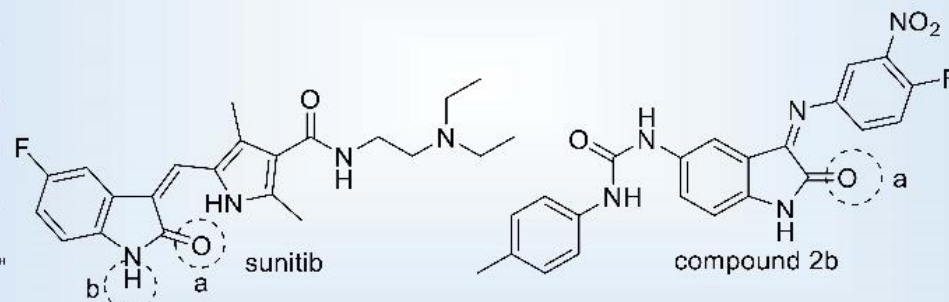
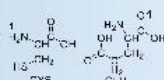
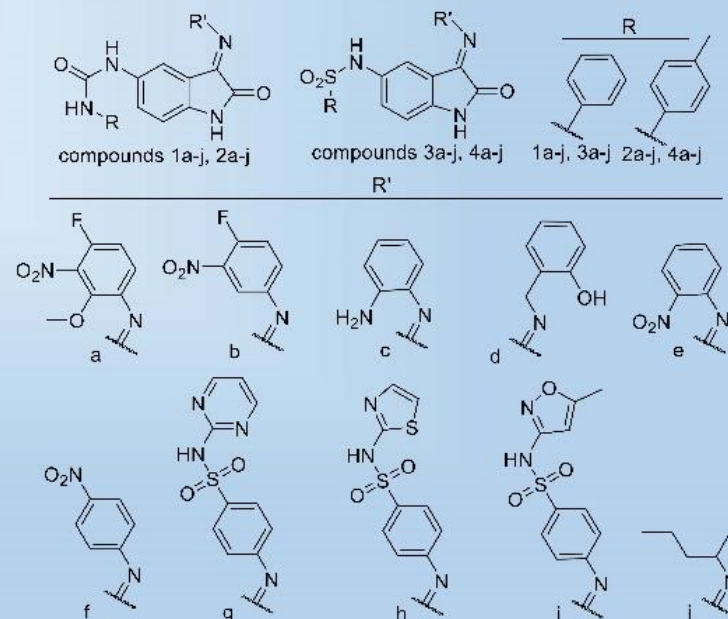


Figure 1. 3D interactions of the compound 2b (colored by atomic type) and **sunitinib** (pink) with VEGFR2



Results: Protein-Ligand interaction plays a significant role in structure-based drug design studies (2). Conformations with the lowest docked energy and RMSD value and highest hydrogen bonding capability were chosen as a strongest binding capability. Most of the compounds showed good binding capability in a range between -9.17 and -14.57 kcal/mol and exhibited interactions with the active site amino acids of CYS919. These compounds also showed better interactions upon urea, sulfonamide or Schiff base groups. Compound **2b** showed the lowest binding energy (-14.57 kcal/mol) with smallest RMSD (0.31°Å).

Conclusions: The results indicate the possibility of the designed compounds may be biologically active due to similar interactions to **sunitinib**

References:

- Kim A, Balis FM, Widemann BC (2009). The Oncologist, 14:805-808.
- Baskaran C, Ramachandran M (2012). Asian Pacific Journal of Tropical Disease, 2:734-738



THE EFFECT OF COX-2 INHIBITORS ON ACETYLCHOLINE ESTERASE IN TREATMENT OF ALZHEIMER'S DISEASE



¹Kahvecioglu D., ²Yilmaz S., ²Yenice-Cakmak G. ¹Kocyigit-Kaymakcioglu B.

¹ Marmara University, Faculty of Pharmacy, Department of Pharmaceutical Chemistry, Istanbul, Turkey.

² Trakya University, Faculty of Pharmacy, Department of Pharmaceutical Chemistry, Edirne, Turkey.

e-mail: dilaykahvecioglu@marun.edu.tr

INTRODUCTION

Alzheimer's disease (AD), which is one of the neurodegenerative diseases affecting millions of people around the world occurs with the degeneration of neurons and loss of neurons (1). Acetylcholine deficiency, aggregation of tau proteins to form neurofibrillary tangles between neurons, extracellular accumulation of β -amyloid ($A\beta$) peptide and oxidative stress play important role formation of AD (2). Today, acetylcholinesterase inhibitors are widely used in the treatment of Alzheimer's disease, which inhibit the hydrolysis of acetylcholine and increase the amount of acetylcholine in the synaptic cleft, but they have limited efficacy and show a variety of dose-related side effects (1). On the other hand, the change of COX activity causes the formation of reactive oxygen species (ROS) and oxidative damage. Elimination of ROS formation may be a new approach to AD treatment (3). For this reason, some COX-2 inhibitors are thought to prevent neuronal damage by suppressing oxidative stress (4).

MATERIAL & METHODS

PREPARATION OF THE PROTEIN

➤ Reaching of the crystal structure of 4EY7 from the Protein Data Bank (PDB)
➤ Optimization and minimization of the protein through extracting the ligand (Donepezil), adding hydrogens by using CHARMM forcefield and ABNR method.
➤ Description the receptor binding site module from the ligand current selection.

PREPARATION OF LIGANDS

➤ 3D-Sketching of the novel compounds and the reference ligand.
➤ Optimization and minimization of ligands by using CHARMM forcefield and ABNR method.

MOLECULAR DOCKING

➤ CDocker method was performed by using Discovery Studio 3.5.
➤ The protein is held rigid while the ligands are allowed to be variable.
➤ The docking and scoring methodology was first validated by docking of known inhibitor and then docking studies were performed on the COX-2 Inhibitors.

ANALYSIS OF RESULTS

➤ Scoring of docking poses by ALP subprotocol and calculating binding energies by CBE subprotocol by using ABNR methods.
➤ The lowest binding energy was taken as the best-docked structure of the compound.

RESULTS & DISCUSSION

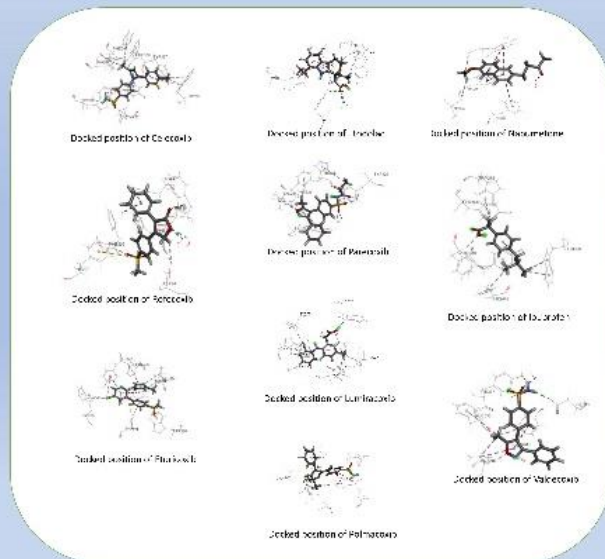
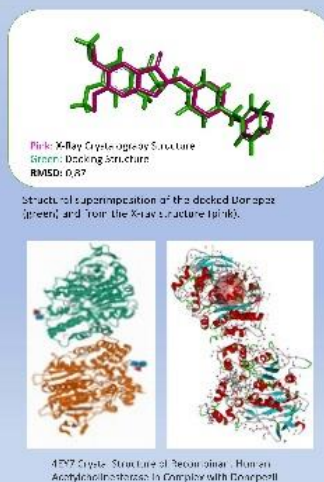
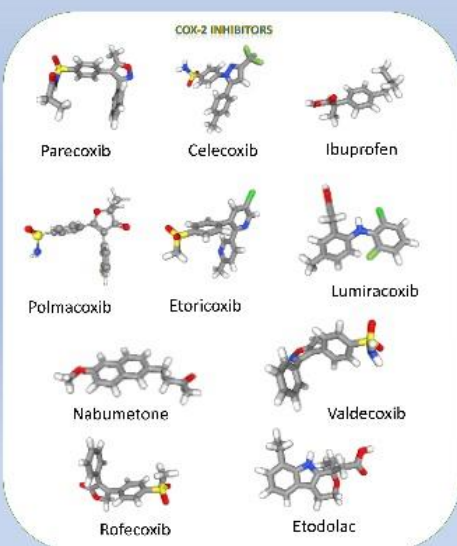


Table 1. Molecular docking results of COX-2 Inhibitors derivatives

Compound Name	Binding Energy	H bonds	Pi Bonds	H bonds via HOH
Donepezil	-150,231	PHE295	TRP86, TRP286, TYR337, PHE338	-
Celecoxib	-67,6958	TYR72, HOH953, HOH955	TYR341, PHE295, TRP86	-
Etodolac	-37,629	SER203, HOH956, HOH955	TYR337, PHE338	TYR341, GLY82 TYR337, ASP74
Nabumetone	-64,2619	SER293, TYR341, HOH955	PHE297, TRP286	-
Lumiracoxib	-49,5601	HOH931, HOH737	TRP286, TYR341, HIS447, TYR72, PHE338	SER125, GLY82, TYR337 ASP74, TYR341
Parecoxib	-50,9515	HOH931, HOH955, HOH737, VAL294, TYR124	TYR341, PHE338, HIS447	SER125, GLY82, TYR377 ASP74, TYR341
Polmacoxib	36,4261	TYR72	TRP286, PHE297, TYR341, VAL294, PHE338	-
Ibuprofen	-55,8079	PHE338, HOH955	TRP286, HIS447, TYR337, TYR341	-
Valdecoxib	-62,654	TYR337, ASP74, VAL294	PHE338, TYR341	SER125
Rofecoxib	-155,273	HOH856, HOH931, HOH956, TRP295	PHE297, PHE338, HIS447, TRP86	GLY82, TYR337, TYR341
Etoricoxib	-100,355	HOH955	PHE338, TRP286, VAL294, TYR341, TYR337, TYR124	-

The interaction of COX-2 inhibitors with acetylcholinesterase enzyme, which is considered as a new approach in the treatment of AD, was investigated with docking studies. Interactions of COX-2 inhibitors with the amino acids Asp74, Trp86, Tyr124, Trp286, Phe295, Tyr337, Phe338 and Tyr341 were revealed. Rofecoxib and Etoricoxib have significant binding energy that can be considered in the treatment of Alzheimer's.

REFERENCES

- Sharma K. (2019). Molecular medicine reports, 20(2), 1479–1487.
- Colović MB, Krstić DZ, et.al. (2013). Curr Neuropharmacol, 11(3):315-35
- Markesbery WR. (1997). Free Radical Biology and Medicine, 23(1), 134-147.
- Song Q, Feng YB, et al., (2019). Neuropharmacology, 160:107779.

INTRODUCTION

Inflammation is the body's defense system response to the stimulation of many factors. Increased vascular permeability, changes in the structure of the membrane and protein denaturation are important factors that trigger the inflammation process. Proteins denaturation is a well-documented reason of inflammation. Therefore, it is recognized that, the compounds that are able to inhibit heat induced protein denaturation, have potential therapeutic remark as anti-inflammatory agents. NSAIDs (Non-steroidal anti-inflammatory drugs) used are also effective by inhibiting albumin denaturation¹.



FIGURE 1 Inflammation pathway.

In this study, by modifying free carboxylic functional group with 1,3,4-oxadiazole, we have designed and synthesized a series of 3,5-disubstituted-1,3,4-oxadiazole derivatives as anti-inflammatory agent with improved activity profile and less side effect^{2,3}.

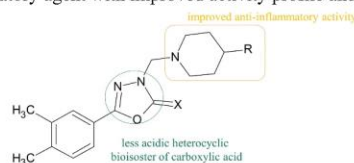


FIGURE 2 Structure of the designed compounds.

CHARACTERIZATION OF THE DESIGNED COMPOUNDS

TABLE 2 Physical and NMR data of the synthesized compounds. M.P.: melting point
All of the compounds gave satisfactory elemental analysis data, which were in full accordance with their depicted structure.

Comp.	Yield (%)	PHYSICAL	IR (KBr, cm ⁻¹)	¹ HNMR (ppm)					
		M.P (°C)	C=X	C=N	Aromatic group	N-CH ₂ -N	piperidin-H ₂ +H ₆	piperidin-H ₃ +H ₅	-CH ₃
4a	71	205.0	1261	1618	7.18-7.37, 8H, m	5.12, s, 2H	2.64-3.30, m, 4H	1.76-1.89, m, 4H	2.34, 6H, s
4b	66	178.8	1251	1622	7.25-7.72, 8H, m	5.12, s, 2H	3.00-3.11, m, 4H	1.77-2.19, m, 4H	2.33, 6H, s
4c	65	111.8	1258	1619	7.09-7.69, 8H, m	5.05, s, 2H	2.44-3.14, m, 4H	1.23-1.67, m, 4H	2.32, 6H, s
4d	62	132.8	1259	1611	7.24-7.71, 3H, m	5.01, s, 2H	2.51-3.23, m, 4H	1.51-2.15, m, 4H	2.33, 6H, s
4e	77	133.9	1776	1629	7.17-7.64, 8H, m	4.75, s, 2H	2.42-3.18, m, 4H	1.76-1.89, m, 4H	2.32, 6H, s
4f	74	177.3	1772	1631	7.21-7.63, 8H, m	4.74, s, 2H	2.97-2.11, m, 4H	1.77-2.17, m, 4H	2.31, 6H, s
4g	31	152.4	1766	1613	7.20-7.60, 8H, m	4.65, s, 2H	2.62-2.97, m, 4H	2.03-2.10, m, 4H	2.31, 6H, s
4h	48	73.4	1752	1627	7.10-7.60, 8H, m	4.68, s, 2H	2.51-3.03, m, 4H	1.47-1.68, m, 4H	2.30, 6H, s
4i	53	124.6	1759	1641	7.06-7.64, 3H, m	4.74, s, 2H	2.62-3.18, m, 4H	1.69-2.28, m, 4H	2.33, 6H, s
4j	32	132.7	1779	1615	7.21-7.62, 8H, m	4.69, s, 2H	2.32-3.12, m, 4H	1.51-2.16, m, 4H	2.31, 6H, s

CONCLUSION

The structure of the newly synthesized 10 compounds was verified by IR and ¹H-NMR spectral methods. The anti-inflammatory activity of the synthesized compounds was investigated using in vitro albumin denaturation assay. All of the compounds gave satisfactory analytical and spectroscopic data, which were in full accordance with their depicted structure. According to *in vitro* biological assays, compounds **4a-c** and **4g-i**, which showed more than 60% inhibition in the albumin denaturation test, were selected for further investigation to elucidate the anti-inflammation mechanism.

SYNTHESIS OF THE DESIGNED COMPOUNDS

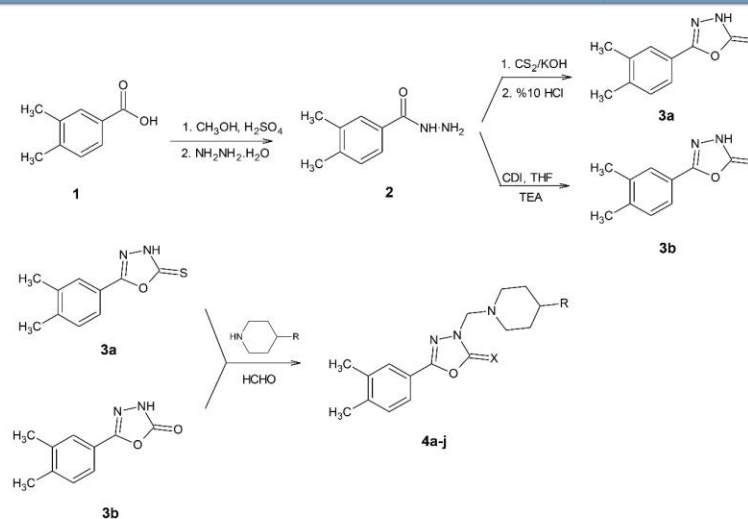


TABLE 1 Structure of the synthesized compounds

No	-X	-R ₁
4a	S	4-Phenyl
4b	S	4-Hydroxy-4-phenyl
4c	S	4-Benzyl
4d	S	4-(4-Morpholine)
4e	O	4-Phenyl
4f	O	4-Hydroxy-4-phenyl
4g	O	4-Acetyl-4-phenyl
4h	O	4-Benzyl
4i	O	4-Cyano-4-phenyl
4j	O	4-(4-Morpholine)

BIOLOGICAL ACTIVITY

The denaturation of tissue proteins and the subsequent production of auto-antigens is one of the well-documented causes of inflammatory and arthritic diseases. Agents that can prevent protein denaturation would therefore be worthwhile for anti-inflammatory drug development. A number of anti-inflammatory drugs are known to inhibit the denaturation of proteins in an *in vitro* screening model for anti-inflammatory compounds⁴.



FIGURE 3 Albumin Denaturation Assay.

The activity test results demonstrated that while indomethacin showed 86.92% activity, compounds **4b** and **4h** showed inhibition activity with 85.53 and 81.03% at 100 µg/mL, respectively. In addition, at the same concentration, compounds **4a**, **4c**, **4g** and **4i** showed more than 60% inhibition activity.

TABLE 3 Albumin denaturation assay results of the compounds

Compound	Activity(%)
Control	100,00
Indomethacin	86,92
4a	67,20
4b	85,53
4c	66,55
4d	25,08
4e	23,20
4f	41,80
4g	69,77
4h	81,03
4i	64,63
4j	56,27

REFERENCE

- Jan MS, Ahmad S, Hussain F, Ahmad A, Mahmood F, Rashid U, Abid O, Ullah F, Ayaz M, Sadiq A (2019). European Journal of Medicinal Chemistry, 186:111863.
- Bhandari, SV, Bothara KG, Raut MK, Patil AA, Sarkate AP, Mokale VJ (2008). Bioorganic & Medicinal Chemistry, 16:1822-1831.
- Ozyazici T, Gurdal EE, Orak D, Sipahi H, Ercetin T, Gulcan HO, Koksak M (2020). Archiv der Pharmazie, 353:2000061.
- Banerjee AG, Das N, Shengule SA, Srivastava RS, Shrivastava SK (2015). European Journal of Medicinal Chemistry, 28:81-95

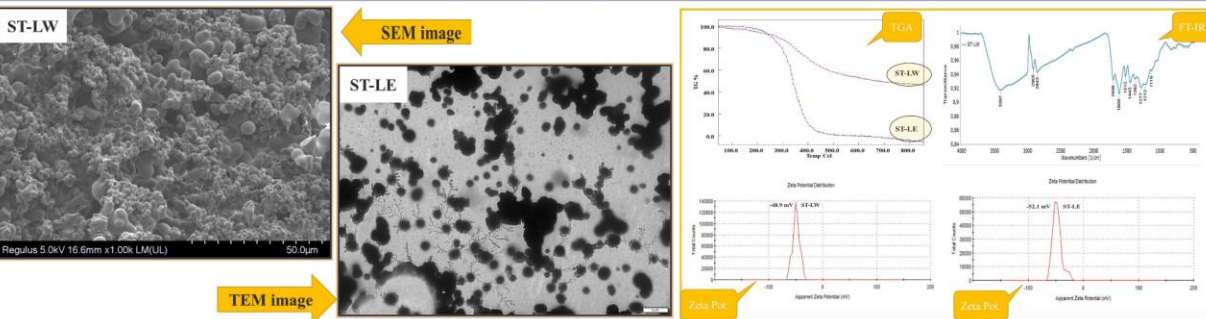
INTRODUCTION

Lavender is a plant species native to the Mediterranean, Middle Eastern countries and the Arabian Peninsula. It is now grown worldwide and has a wide variety of pharmacological properties as a result of the essential oil of its flowers. Lavender has complex chemical compositions, especially rich with lipophilic components (essential oil) and hydrophilic components (phenolic compounds, anthocyanins, phytosterols, tannins, flavone glycosides, etc.). There has been a recent increase in the popularity of plant-based natural products as potential therapeutic agents for modern and alternative complementary medicine. The studies conducted so far have focused on the direct application of extracts or the production of metal nanoparticles with these extracts. However, today, using the hydrothermal method, nano / microparticles of herbal ingredients can be made directly, apart from standard methods. In this way, it can be shown that the particle forms may have a higher effect in various applications, even if the direct effects of the active ingredients have not been determined. For this purpose, in this study, microparticles were synthesized from lavender extracts using two different solvents and their cytotoxic and genotoxic effects on Malign melanoma cell line (SK-MEL), human breast (MCF-7) and lung cancer (A549) cells were investigated.

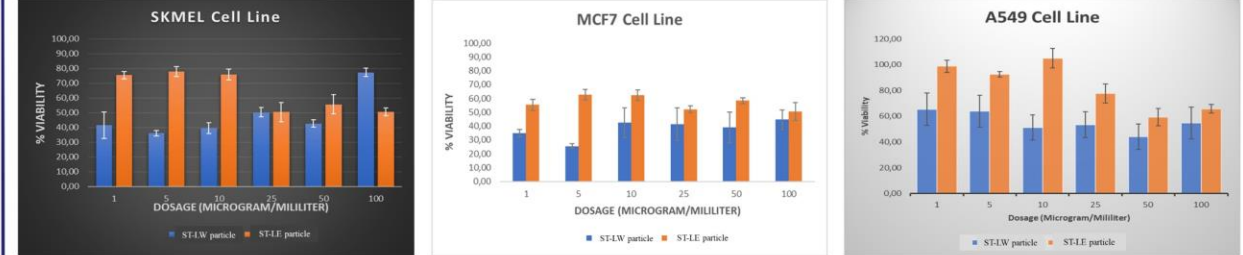
PREPARATION OF LAVENDER MICROPARTICLES WITH HYDRO/SOLVOTHERMAL SYNTHESIS



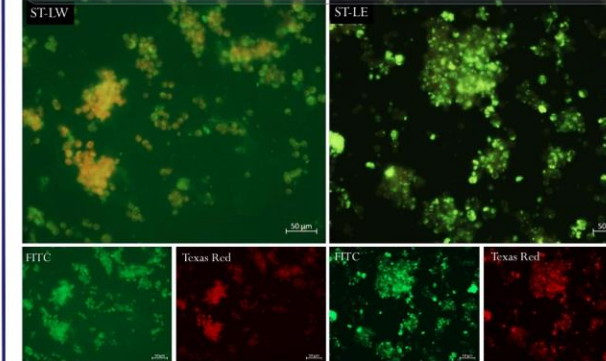
CHARACTERIZATION OF LAVENDER MICROPARTICLES



CELL CULTURE STUDY



SK-MEL CELL LINE



MCF-7 CELL LINE

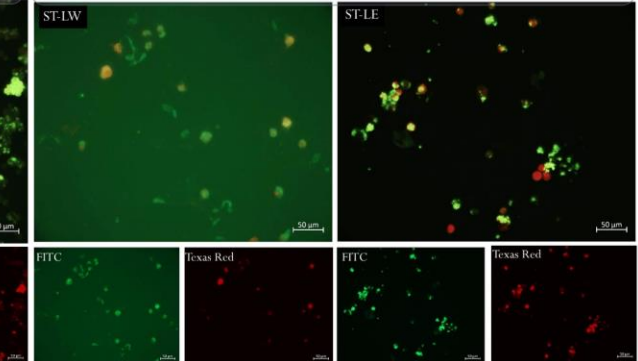


Table 1: Genotoxic evaluation of the Lavender extract with water and ethanol

Material	Dosage (µg/mL)	Counted Cells	Average MN (%)	Average CPI (%)
A549 Cell	-	2000	1.49	0.25±0.01
Solvent Control (water)	-	2000	1.28	0.18±0.02
STLE	100	2000	1.73	0.27±0.07
STLW	100	2000	1.79	0.27±0.05

CONCLUSION

- ❖ Lavender extracts have been prepared by using water and ethanol extract.
- ❖ Micro sized particles have been synthesized successfully by using hydro/solvothermal synthesis.
- ❖ Characterization was realized by using SEM, TEM, TGA, FT-IR, zeta potential, confocal mic.
- ❖ Cytotoxicity results of the particles on different cancer lines have been shown. ST-LW particles had good cytotoxic effect than ST-LE. Both particles, ST-LW and ST-LE have no genotoxic effect.

SYNTHESIS AND STANDARDIZATION OF AN IMPURITY OF ACETAMINOPHEN, DEVELOPMENT AND VALIDATION OF RELATED ULTRA-HIGH PERFORMANCE LIQUID CHROMATOGRAPHIC METHOD

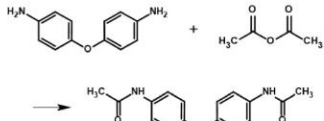
Cemil Caner Arıkan¹, İlkyay Küçükgüzel²

¹ Atabay Pharmaceuticals and Fine Chemicals Inc., Acıbadem Plant and Headquarters, Kadıköy 34718 İstanbul, Turkey
² Marmara University, Faculty of Pharmacy, Department of Pharmaceutical Chemistry, Haydarpaşa 34668 İstanbul, Turkey
canerarikan@marun.edu.tr

Introduction

Acetaminophen (*N*-(4-Hydroxyphenyl)acetamide) also known as paracetamol is a common analgesic and antipyretic drug used for the relief of fever, aches and pains [1,2]. When acetaminophen is analyzed by HPLC according to organic impurities analysis method of acetaminophen in American Pharmacopoeia Version 42 (USP 42) [3], an impurity molecule is observed on the chromatogram which is not defined by the USP 42. We identified this impurity molecule as *N,N'*-[Oxydi(4,1-phenylene)]diacetamide (ODAA) by LC-MS/MS and other studies. In the present work, this molecule was synthesized, characterized, standardized and the current HPLC method for organic impurities analysis of acetaminophen was transferred to UHPLC by developing a new related method including this impurity. The method was validated according to international conference on harmonization (ICH) guideline [4] and stress-test studies of acetaminophen were performed with forced degradation studies.

Methods | Synthesis and Characterization



N,N'-[Oxydi(4,1-phenylene)]diacetamide (ODAA) was synthesized by dissolving 4,4'-Oxydianiline in acetone at 0°C and adding acetic anhydride dropwise and the reaction was carried out for 3h at 0°C. For crystallization, the obtained ODAA was completely dissolved in ethanol and the final solution was evaporated. The synthesized ODAA was identified by the use of IR, ¹H-NMR, ¹³C-NMR, HMBIC NMR, HPLC, LC-MS/MS, elemental analysis and melting point determination.

Table 2: NMR results of ODAA.

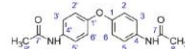


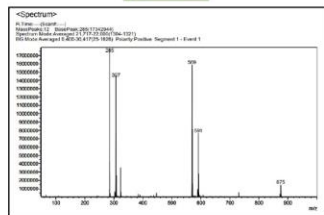
Figure 1: Synthesis of ODAA.

- Yield: 95%
- Melting Point: 230°C.
- Appearance: White crystalline powder.
- Solubility: Soluble in ethanol, methanol and DMSO.

Table 1: Elemental analysis of ODAA.

Element	Amount by mass (%)	
	Calculated	Found
Carbon (C)	67.590	66.890
Hydrogen (H)	5.670	5.582
Nitrogen (N)	9.850	9.849

Q3 Scan Mode



- 285 m/z: ODAA + 1H (284+1=285 g/mol)
- 307 m/z: ODAA + Na (284+23=307 g/mol)
- 569 m/z: ODAA dimer (284x2)+1H=569 g/mol)
- 591 m/z: ODAA dimer + Na (284x2+23=591 g/mol)
- 875 m/z: ODAA trimer+Na (284x3+23=875 g/mol)

Product ion scan of 285 m/z

Product Ion Scan Mode

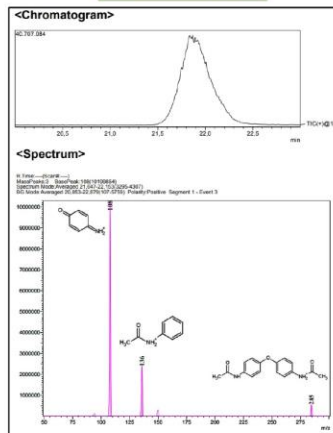


Figure 2: Results of LC-MS/MS.

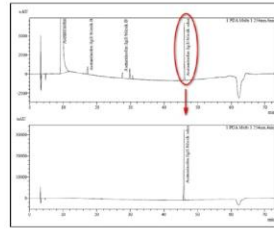


Figure 3: HPLC chromatograms of acetaminophen sample solution and ODAA solution.

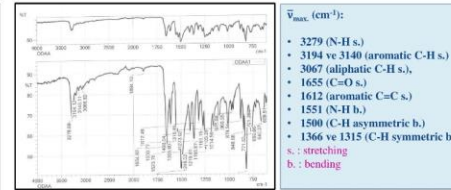


Figure 4: IR spectrum of ODAA.

Standardization of ODAA

The potency of the synthesized ODAA molecule was calculated with the help of the following formula [5] and the results found in Table 3:

Table 3: Results for calculating the potency of ODAA.

Analysis	Method	Results
Organic Impurities	HPLC	%0.010000
Inorganic Impurities	Residue on Ignition (Sulfated Ash)	%0.009946
Residual Solvents	GC	%0.037027
Water Content	Karl Fischer	%0.305000

$$\text{Potency (\%)} = 100\% \times \frac{100\% - \% \text{ impurities}}{100} \times \frac{100\% - (\% \text{ water} + \% \text{ residual solvents} + \% \text{ others})}{100}$$

$$\text{Potency (\%)} = 100\% \times \frac{100\% - 0.01\%}{100} \times \frac{100\% - (0.305\% + 0.037027\% + 0.009946\%)}{100}$$

The potency of the synthesized ODAA molecule was calculated using the results above and found to be 99.64%.

UHPLC Method Development

Method development studies were performed on the Shimadzu Nexera X2 model ultra-high performance liquid chromatography (UHPLC) system equipped with a photodiode array detector.

Table 4: Chromatography system conditions for the UHPLC system.

Chromatography	Ultra-High Performance Liquid Chromatography (UHPLC)
Detector	UV 254 nm
Column	Inertsustain C8, 150 × 2.1 mm, 2-μm
Flow	0.2 mL/min
Column Temperature	40°C
Injection Volume	1 μL
Run Time	30 min.

Table 5: Mobile phase program for gradient elution (UHPLC).

Time (min.)	Solvent A (%)	Solvent B (%)
0	65	35
1	65	35
6	22	78
22	22	78
25	65	35
30	65	35

Validation

Table 6: System suitability results of the UHPLC method.

Substance	Tailing Factor (T)	Resolution (R)	RSD %
Acetaminophen	1.203	1.091	0.429
Acetaminophen related compound B	1.091	1.203	0.448
Acetaminophen related compound C	1.065	1.252	0.433
Acetaminophen related compound D	1.038	1.011	0.414
Acetaminophen related compound J	1.011	1.011	0.418
ODAA	1.037	1.037	0.421

Table 7: Acetaminophen impurity limits and specificity results of the UHPLC method.

Substance	Limit (max. %)	Retention Time (RT) (min)	Relative Retention Time (RRT)	Peak Purity Index	Single Peak Threshold
Acetaminophen	-	4.492	1.000	1.0000	0.941000
Acetaminophen related compound B	0.050	7.335	1.634	1.0000	0.780211
Acetaminophen related compound C	0.050	9.061	2.016	1.0000	0.870001
Acetaminophen related compound D	0.050	11.831	2.645	1.0000	0.650209
Acetaminophen related compound J	0.001	20.649	4.597	1.0000	0.837009
ODAA	0.050	21.333	4.759	1.0000	0.918711

Table 8: Precision results of the UHPLC method.

Substance	System Precision		Method Precision	
	RSD % (Peak areas, n=6)	RSD % (Retention times, n=6)	Amount % (n=6)	RSD % (n=6)
Acetaminophen	0.429	0.363	-	-
Acetaminophen related compound B	0.448	0.369	0.04994	0.472
Acetaminophen related compound C	0.433	0.352	0.04628	0.467
Acetaminophen related compound D	0.414	0.350	0.04847	0.459
Acetaminophen related compound J	0.918	0.353	0.00102	1.217
ODAA	0.421	0.368	0.04940	0.383

Table 10: Results of regression analysis of the linearity data of acetaminophen and its impurities.

Substance	Range (μg/mL)	Slope	Intercept	r ²	LOD (μg/mL)	LOQ (μg/mL)
Acetaminophen	1.248-24.960	18082.420	-4345.891	0.9998	0.374	1.248
Acetaminophen related compound B	0.373-24.885	132262.500	415.7807	0.9994	0.124	0.373
Acetaminophen related compound C	1.217-24.347	60158.66	324.0392	1.0000	0.365	1.217
Acetaminophen related compound D	0.369-24.611	152303.00	703.5019	1.0000	0.123	0.369
Acetaminophen related compound J	0.125-0.499	263825.00	-88.31898	0.9999	0.050	0.125
ODAA	0.373-24.850	333330.00	685.3543	0.9983	0.124	0.373

Table 12: Degradation results of acetaminophen.

Stress condition	Time (day)	% Assay of the impurities					Total impurities	Total impurities
		Imp-B*	Imp-C*	Imp-D*	Imp-J*	ODAA degradation		
Acidic hydrolysis (0.5 N HCl)	0	0.0018	ND	ND	ND	≤LOQ	0.018	0.018
	15	≤LOQ	ND	ND	ND	≤LOQ	0.018	0.018
Alkaline hydrolysis (0.5 N NaOH)	0	0.0018	ND	ND	ND	≤LOQ	0.018	0.018
	15	≤LOQ	ND	ND	ND	≤LOQ	0.018	0.018
Oxidative degradation (3.0% H ₂ O ₂)	0	0.0018	ND	ND	ND	≤LOQ	0.018	0.018
	15	0.0020	ND	ND	ND	≤LOQ	0.018	0.018
Thermal degradation (Dry heat, 60°C ± 2°C)	0	0.0018	ND	ND	ND	≤LOQ	0.018	0.018
	15	0.0018	ND	ND	ND	≤LOQ	0.018	0.018
Photolytic degradation (UV light, 254 nm)	0	0.0018	ND	ND	ND	≤LOQ	0.018	0.018
	15	0.0019	ND	ND	ND	≤LOQ	0.019	0.019

* Imp-B: Acetaminophen related compound B, Imp-C: Acetaminophen related compound C, Imp-D: Acetaminophen related compound D, Imp-J: Acetaminophen related compound J, ND: not detected

Results and Discussion

An undefined impurity molecule of acetaminophen in USP 42 was synthesized, characterized, standardized and an UHPLC method including this impurity was developed for the analysis of organic impurities of acetaminophen. Requirements for the validation study of the developed method were fulfilled according to ICH. The validated UHPLC method has been proved to be sensitive, selective, precise, linear, accurate and robust. The developed method provides a good resolution between acetaminophen, acetaminophen related compound B, acetaminophen related compound C, acetaminophen related compound D, acetaminophen related compound J and ODAA, and could be used for determination of organic impurities of acetaminophen. Compared to the related method in USP 42, the new developed UHPLC method offers a short analysis time and uses less mobile phase.

Acknowledgements

The authors are thankful to Marmara University, Faculty of Pharmacy, Department of Pharmaceutical Chemistry, Istanbul, Turkey and Atabay Pharmaceuticals and Fine Chemicals, Istanbul, Turkey, for letting use of their laboratories, chemicals and instruments.

References

- M. Espinosa Bosch, A.J. Ruiz Sánchez, F. Sánchez Rojas, C. Bosch Ojeda, Determination of paracetamol: Historical evolution, J. Pharm. Biomed. Anal. 42 (2006) 291-321.
- M.J. O'Neil (ed.), The Merck Index: An encyclopedia of chemicals, drugs, and biologicals, 13th ed. (2001), Merck and Co., Inc., Whitehouse Station, New Jersey, USA.
- United States Pharmacopoeia 42, Volume 1: Official Monographs: Acetaminophen, American Pharmacopoeial Convention, 12601, Twinbrook Parkway, Rockville, MD 20852, 2020; p40-42.
- ICH Topic Q2 (R1): Validation of Analytical Procedures: Text and Methodology, Step 5. Note For Guidance On Validation of Analytical Procedures: Text And Methodology, CPMP/ICH/381/95, European Medicines Agency, 1995.
- D.K. Singh, S. Sharma, A. Thakur, S. Kumar, S. Singh, Pharmaceutical analysis - Drug purity determination. In: P. Worsfold, A. Townsend, C. Poole, M. Miro, eds. Encyclopedia of Analytical Science, 3rd ed. Elsevier Ltd. (2019) 188-199.